BMC Ophthalmology

SYSTEMATIC REVIEW Open Access

A comprehensive overview: deep learning approaches to central serous chorioretinopathy diagnosis

Mohammad Shojaeinia[1], Azamossadat Hosseini[1], Mostafa Naderi[2], Bardia Baloutch[3], Mohammad Shokoohi Yekta[4], Leila Akbarpour[5] and Hamid Moghaddasi[1*]

Abstract

Purpose To synthesize evidence on deep learning applications for diagnosing central serous chorioretinopathy (CSCR), a macular disorder associated with vision loss, this systematic review categorized studies by diagnostic task and imaging modality. The study evaluates advances in deep learning performance, clinical integration potential, dataset limitations, and the contributions of multimodal imaging and Explainable AI (XAI) to diagnostic accuracy and clinical decision-making.

Methods We conducted a PRISMA-compliant systematic review of PubMed, Scopus, and IEEE Xplore, including peer-reviewed English-language studies published from January 1990 to February 2024 that reported quantitative deep learning metrics for CSCR diagnosis. A two-stage selection process was applied (Cohen's $\kappa = 0.84$), resulting in 96 studies for analysis. Risk of bias was evaluated using the QUADAS-2 tool, and data were synthesized by imaging modality, model architecture, and diagnostic task.

Results Deep learning models demonstrate exceptional performance in CSCR diagnosis. DenseNet architectures applied to optical coherence tomography (OCT) images achieved peak Metrics, including 99.78% accuracy, 99.68% sensitivity, and 100% specificity. Segmentation models for subretinal fluid (SRF) reported Dice scores of up to 0.965, while multimodal models for differential diagnosis achieved an area under the curve (AUC) of 0.999. Despite these advances, clinical adoption remains limited by several challenges: scarce and imbalanced datasets (e.g., SRF/non-SRF ratio of 1:8), lack of open-access datasets and models, risks of overfitting, and insufficient external validation. Emerging approaches, such as few-shot learning and diffusion models, are promising for mitigating data constraints; however, improvements in dataset quality and the implementation of rigorous cross-institutional validation are essential for real-world deployment.

Conclusions By leveraging OCT and multimodal imaging data, deep learning has the potential to transform CSCR diagnosis through enhanced accuracy and automation. However, translating these advances into routine clinical practice necessitates overcoming key challenges, including limited and heterogeneous datasets and models with restricted generalizability. Future research should prioritize standardized reporting frameworks, transparent

*Correspondence:
Hamid Moghaddasi
moghaddasi@sbmu.ac.ir

Full list of author information is available at the end of the article

model interpretability through XAI, and rigorous large-scale validation. Essential strategies include employing federated learning to leverage distributed data, implementing effective multimodal fusion techniques, and fostering collaborative frameworks to improve diagnostic accuracy, ensure algorithmic fairness, and enable real-world clinical applicability.

Keywords Diagnosis, Retinopathy, Central serous chorioretinopathy, Artificial intelligence, Machine learning, Deep learning

Background

Central serous chorioretinopathy (CSCR) is a macular disorder characterized by subretinal fluid (SRF) accumulation, often accompanied by pigment epithelial detachment (PED). This results in neurosensory retinal detachment and visual impairment. The diagnosis of this condition remains challenging due to the variable presentations of the disease, the overlap with other retinal diseases, and the limitations of conventional imaging interpretation. Advancements in imaging modalities, including but not limited to optical coherence tomography (OCT), fundus fluorescein angiography, and indocyanine green angiography, have led to significant progress in the visualization of CSCR. However, manual interpretation is a time-consuming process that is also subjective and prone to variability. This has led to an increased interest in artificial intelligence (AI) and deep learning (DL) for the automated diagnosis of Medical conditions. This review synthesizes evidence on DL applications for CSCR diagnosis, focusing on Model performance, imaging modalities, and clinical integration. A systematic search of PubMed, Scopus, and IEEE Xplore yielded 96 studies (January 1990–February 2024) reporting quantitative Metrics for DL-based CSCR diagnosis. The studies were then categorized based on their diagnostic task, which included classification, segmentation, differential diagnosis, and prognosis. Bias assessment of the studies was conducted using the Quality Assessment of Diagnostic Accuracy Studies 2 (QUADAS-2) tool. Despite the high accuracies reported for models such as DenseNet and EfficientNet on OCT images, their clinical adoption is limited by several factors. These include dataset scarcity, class imbalance, a lack of external validation, and limited interpretability. Emerging approaches, including multimodal fusion, few-shot learning, and diffusion models, show promise but require further validation. This review underscores the need for standardized reporting, diverse datasets, and collaborative frameworks to enable clinically applicable, interpretable, and ethically sound DL-based CSCR tools.

Introduction

Clinical background of CSCR

CSCR is a macular disorder characterized by the accumulation of SRF, leading to neurosensory retinal detachment, often accompanied by pigment epithelial detachment (PED) [1–4]. It is the fourth most common retinopathy after age-related macular degeneration (AMD), diabetic retinopathy (DR), and retinal vein occlusion (RVO), predominantly affecting individuals aged 30–50 years [5]. The prevalence is approximately 9.9 per 100,000 in Males and 1.7 per 100,000 in females [6]. Although the precise etiology remains unclear [7] factors such as psychological stress, corticosteroid use, and genetic predisposition have been implicated [8]. Common clinical manifestations include central vision distortion, blurred vision, central scotoma, altered color perception, micropsia, and metamorphopsia.

Pathophysiology and risk factor

In addition to subretinal fluid (SRF) accumulation, the underlying pathophysiology of CSCR involves choroidal hyperpermeability, vascular dysfunction, and systemic influences [9]– [10]. Corticosteroid use and psychological stress, associated with elevated cortisol and epinephrine levels, contribute to dysregulation of choroidal vascular tone. This dysregulation increases hydrostatic and osmotic pressures, leading to vascular congestion, choroidal thickening, and impaired autoregulation of choroidal circulation. These alterations result in increased vascular permeability, weakening of retinal pigment epithelium (RPE) tight junctions, and disruption of the blood–retina barrier, ultimately causing fluid leakage beneath the RPE and SRF accumulation [11–17]. Furthermore, irregular PEDs have been linked to genetic susceptibility, including variants associated with AMD [18]. Advances in imaging, such as OCT angiography (OCTA), and artificial intelligence (AI) applications [19] have deepened understanding of these mechanisms, while steroid withdrawal and stress management remain therapeutic mainstays. In the future, research should focus on the integration of genetic profiling with multimodal AI analytics [20]. This integration will enable personalized CSCR care, enhancing therapeutic efficacy and patient outcomes.

Diagnostic process

In CSCR, SRF spontaneously resolves in most acute cases; however, persistence beyond several months can result in outer retinal damage, chronic disease progression, and choroidal neovascularization (CNV) [11]–[12]. A substantial body of research has indicated that

approximately 12.8% of patients may experience permanent visual impairment or blindness due to inadequate disease management and SRF-induced damage to the RPE and photoreceptors [21]. Consequently, timely and accurate diagnosis is imperative for effective management. CSCR evaluation entails a meticulous appraisal of symptoms, medical and surgical history, and imaging findings [see Appendix A]. However, the presence of subclinical manifestations and inherent variability complicates the diagnostic process [22].

Imaging modalities in CSCR

Imaging is vital for diagnosing, monitoring, and managing CSCR. Different imaging methods provide complementary insights into disease characteristics, treatment response, and differentiation from other retinal disorders. The following summarizes key imaging techniques commonly used to evaluate CSCR.

- Optical coherence tomography (OCT): is a non-invasive imaging technique that produces high-resolution, cross-sectional images of the retina, enabling diagnosis and management of macular diseases, including CSCR [2]. Ophthalmologists can visualize and measure the thickness of individual retinal layers, and sequential OCT scans allow monitoring of disease progression and treatment response. OCT is a particularly valuable diagnostic tool for distinguishing CSCR from pachychoroid neovasculopathy (PNV) and polypoidal choroidal vasculopathy (PCV) [23]. High-resolution swept-source OCT (SS-OCT) enables enhanced visualization of deeper ocular structures, including the choroid [24]– [25].
- Color fundus photography (CFP): is a widely used method for capturing digital images of the retina [26]. However, SRF and RPE changes are often challenging to detect through funduscopic examination.
- Fundus autofluorescence (FAF): is a non-invasive diagnostic adjunct used to detect CSCR. FAF images typically reveal hyperfluorescence in areas of atrophy and neurosensory retinal detachment caused by SRF and RPE changes, providing critical insight into the pathophysiology of CSCR. In chronic cases, FAF effectively highlights RPE damage [27–31].
- Indocyanine green angiography (ICGA): is an imaging technique that utilizes infrared light to detect choroidal vascular abnormalities and evaluate areas of choriocapillaris nonperfusion [32]– [33].
- Fundus fluorescein angiography (FFA): is a well-established diagnostic tool for CSCR. This technique utilizes time-lapse imaging to assess structural and hemodynamic changes in the retinal vasculature, detect leakage, and identify vascular occlusions. CSCR can be distinguished from other retinal diseases by characteristic FFA patterns, such as the 'smoke stack' or 'inkblot' appearance [34]– [35].
- Optical coherence tomography angiography (OCTA): is a non-invasive imaging technique that visualizes the retinal and choroidal vasculature [36]– [37]. Relative to FFA, OCTA is faster and does not require the administration of exogenous dye.

Table 1 Imaging modalities alongside cscr's hallmark findings

Modality	Features	Clinical Applications	Limitations
OCT	High-resolution cross-sectional	SRF/PED measurement	Limited leakage point localization; artifacts in hemorrhage
CFP	Digital retinal images	Early RPE changes	Poor SRF visualization
FAF	Hyperfluorescence area	Highlighting atrophic or detachment-related fluorescence patterns.	Not applicable for structural analysis.
ICGA	Choroidal vasculature	Hyperpermeability detection	Iodine allergy contraindications; no quantitative standards
FFA	Time-lapse sequences	"Smokestack" leakage patterns	Invasive dye risk; poor choroidal detail
OCTA	Dye-free capillary imaging	Choriocapillaris flow	Signal attenuation in pigmented RPE

The key characteristics, diagnostic utility, and modality-specific limitations relevant to imaging-based CSCR diagnosis are summarized in Table 1.

A notable limitation of OCT in CSCR diagnosis is its inability to precisely localize leakage points, which are imperative for confirming the diagnosis and guiding treatment. In contrast, FFA offers precise identification of leakage points [19]. In acute CSCR, the retinal pigment epithelium (RPE) is typically relatively intact [38]. The primary purpose of FFA is to enhance visualization of the retinal vasculature, facilitating differentiation between acute and chronic CSCR [39]. Both FFA and ICGA are critical for accurate diagnosis, and their combined use can detect polyps in polypoidal choroidal vasculopathy (PCV) or ischemic changes in diabetic macular edema (DME). Consequently, a multimodal imaging approach is essential for comprehensive assessment of choroidal and RPE status [40]– [41].

Diagnostic challenges

Conventional diagnostic methods for CSCR mainly rely on manual image interpretation [4, 20]. This approach

is subjective, time-consuming, and affected by inter-observer variability, making diagnostic consistency difficult [42–47]. Traditional techniques also struggle to detect early-stage disease, quantify changes during disease progression or treatment, and monitor shifts in subretinal fluid or retinal structure over time [3, 42]– [43, 48]. These limitations can delay diagnosis and hinder optimal treatment decisions [4, 22, 42–47]. As a result, clinical practice is increasingly turning to advanced imaging modalities and automated systems that integrate multiple imaging sources. Conventional image processing and classical machine learning are predicated on handcrafted features and exhibit inconsistent generalizability [49]. Deep learning is a promising approach that uses multilayer neural networks to find complex patterns in data. This can lead to more reliable and automated CSCR diagnosis.

Rationale for deep learning integration

Deep learning models facilitate automated and objective solutions, enhancing diagnostic accuracy and enabling early intervention [25–27]. These models can identify features associated with CSCR, such as SRF, PED, variations in choroidal thickness, and disruptions in the outer retinal layers as observed on OCT. Additionally, they assist in detecting changes in the RPE and serous retinal detachment on CFPs, choroidal hyperpermeability on ICGA, and leakage points on FFA. Convolutional neural networks (CNNs) represent the most widely adopted deep learning method for automating the diagnosis of CSCR in retinal images. This approach reduces dependence on subjective interpretation and facilitates earlier, more effective intervention [50–52]. CNNs demonstrate high accuracy in segmenting SRF and PED, which are essential features for CSCR diagnosis, with Dice coefficients consistently exceeding 0.95. These particular deep learning networks are structured to learn spatial hierarchies of features, progressing from low- to high-level representations. The architecture of CNNs is inspired by the organizational structure of the animal visual cortex [53]. As illustrated in Fig. 1, CNN architectures typically include convolutional layers to extract hierarchical features from input images, pooling layers for dimensionality reduction, and fully connected layers for classification or regression.

Methods

Literature search and Article selection

A PRISMA-compliant systematic review was conducted (Fig. 2). Databases (PubMed, Scopus, IEEE Xplore) were searched using the following terms: "central serous chorioretinopathy," "deep learning for CSCR diagnosis," "artificial intelligence in ophthalmology," "retinal image analysis," "optical coherence tomography (OCT)," "color fundus photography (CFP)," "Fundus fluorescein angiography (FFA)," "fundus autofluorescence (FAF)," "indocyanine green angiography (ICGA)," and "multimodal images".

Inclusion criteria

We included studies that utilized deep learning for the diagnosis of CSCR from retinal images, reported quantitative performance metrics (e.g., accuracy, AUC, Dice coefficient), and were peer-reviewed articles published in English between 1990 and 2025.

Exclusion criteria

Non-English studies, non-quantitative reports, and non-CSCR retinal diseases were excluded from the analysis. Quantitative metrics objectively assess deep learning model performance. Excluded studies lacked these metrics to maintain methodological consistency and allow

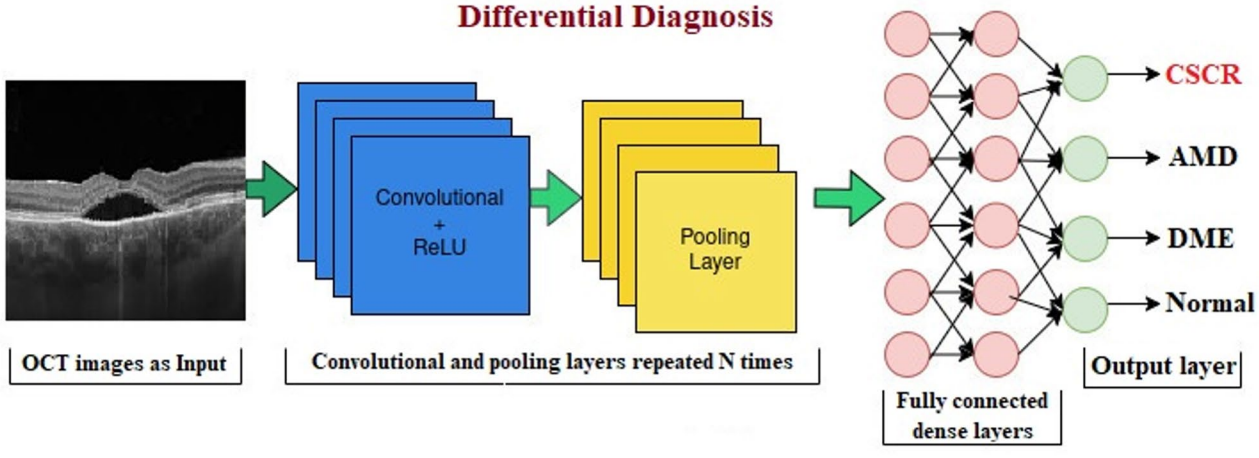

Fig. 1 Typical architecture of a CNN for a classification task

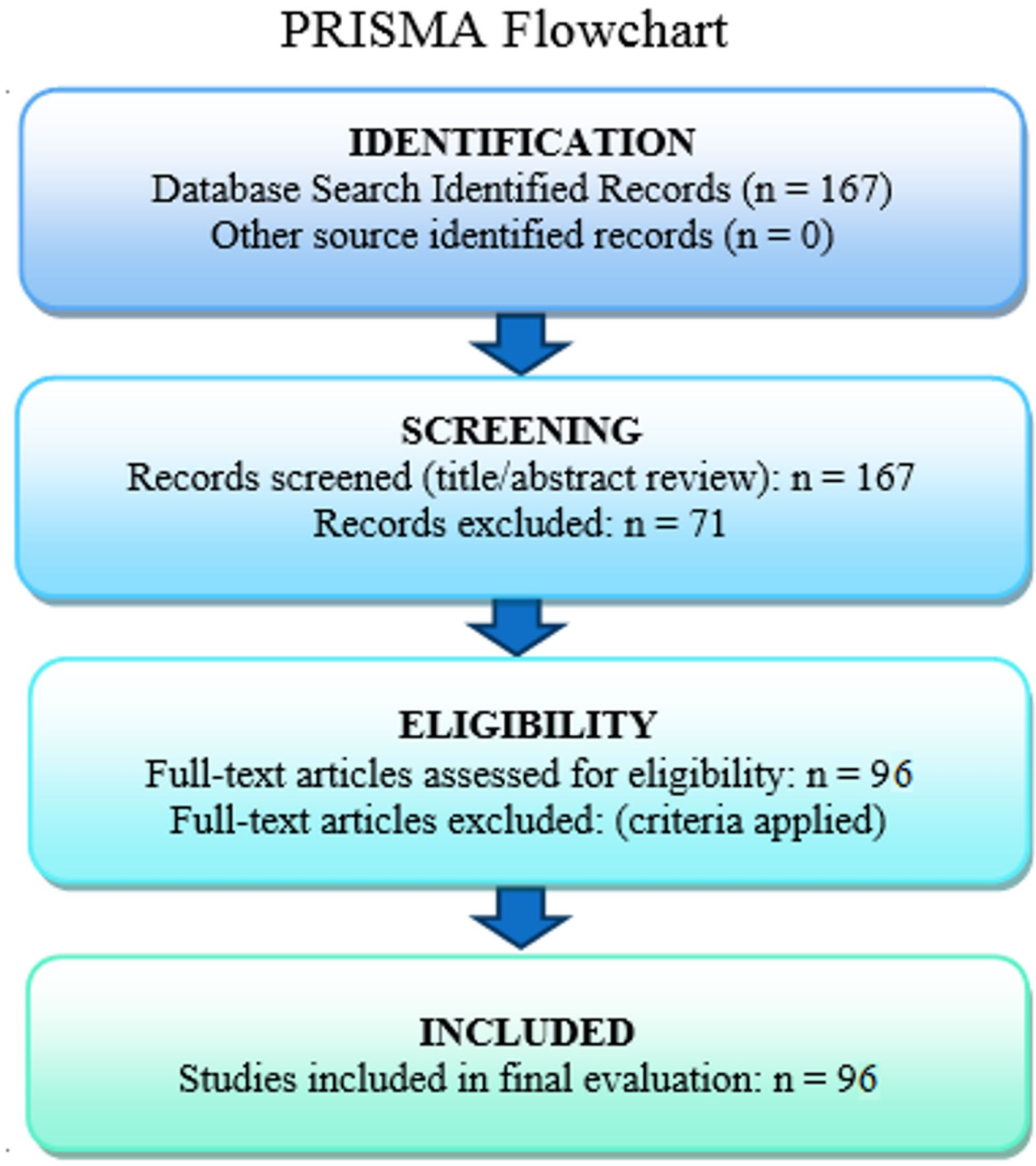

Fig. 2 PRISMA flowchart of the study selection

for a robust comparison of results. The review was restricted to English-language articles to ensure accurate interpretation of study details. This was necessary due to resource constraints and the potential for linguistic biases in data extraction and interpretation.

Inter-Reviewer agreement

A two-stage process, involving title and abstract screening by two independent investigators, resulted in 96 articles from 167 initial articles being selected for final evaluation (Cohen's $\kappa = 0.84$), indicating a high level of inter-reviewer agreement.

Risk-of-Bias assessment

To ensure methodological rigor and transparency, a risk-of-bias (RoB) assessment was conducted for the 96 studies included in this systematic review. The evaluation employed the QUADAS-2 (Quality Assessment of Diagnostic Accuracy Studies) framework, adapted for AI-based diagnostic research with additional criteria addressing dataset quality, model validation, and reproducibility. The QUADAS-2 analysis revealed the following results: overall, 28% (27/96) of studies were rated as low risk, 33% (32/96) as high risk, and 39% (37/96) as unclear risk. Domain-specific assessments indicated high-risk proportions in Patient Selection (65%), Index Test (35%), and Reproducibility (82%).

Data extraction and analysis

The following data were extracted: imaging modalities, deep learning architectures, datasets, and performance metrics. The narrative synthesis entailed a systematic integration of findings to provide a coherent understanding of the applications of deep learning in diagnosing CSCR. The identification of key challenges and limitations in each study was documented to highlight research gaps [54–58]. The studies were subsequently categorized by tasks, which included classification (binary/multi-class), segmentation, differential diagnosis, and prognosis. The studies were then grouped by themes, including binary classification, segmentation, differential diagnosis, and prognostic monitoring. Each study in a given category was subjected to analysis, and contributions were systematically organized by input type, sub-task, and methodology. A tabular presentation of the methods, datasets, and model performance metrics was also made. The findings were interpreted in the context of clinical applications, scalability, and model integration into diagnostic workflows. Finally, future research directions to enhance the diagnostic accuracy of CSCR using deep learning were discussed.

Results

Multiple methodologies have been employed for CSCR diagnosis, including Vision Transformers (ViTs) [48] Capsule Networks [59]and image processing techniques such as discrete wavelet transform (DWT) and local binary patterns (LBP) [60]. Classical machine learning algorithms, such as support vector machines (SVM), random forests (RF), and logistic regression (LR), as well as multimodal fusion models [61]have also been investigated. Deep learning models demonstrate superior performance, achieving high diagnostic accuracy and computational efficiency. Reported applications include segmentation, diagnostic classification, prognostic prediction, and feature extraction. Figure 3 illustrates the range of CSCR research approaches, from screening to subtype classification.

Comparative tabular summaries of methodologies, datasets, input modalities, and performance metrics provide a comprehensive overview of the current state of the art in CSCR diagnosis and management.

Datasets overview, sources, quality, and class distribution

The referenced studies utilize a mix of public, clinical, and proprietary datasets, primarily drawn from OCT, CFP, FFA, and FAF imaging modalities. Public datasets like OCTID [45] consist of a public OCT dataset with 934 images (normal: 618, CSCR: 306) and the Retinal Fundus Multi-Disease Image Dataset (RFMiD) [62]which contains public CFPs for CSCR classification. Clinical datasets are collected from hospitals, including Hangil Eye Hospital and Zhejiang University Hospital. In-house collections encompass custom datasets for specific studies, as evidenced by works such as Zhou et al. and Xu et al. Preprocessing techniques reported in CSCR-related studies frequently include noise reduction (e.g., median filtering), contrast enhancement through histogram equalization, and geometric adjustments such as cropping and resizing. Data augmentation strategies, including rotation and flipping, are widely employed to mitigate overfitting. More advanced approaches involve denoising algorithms [59] and systematic exclusion of low-quality images [19]. Acquisition protocols, including high-quality en-face OCT [63] and 1- and 7-line raster scans [43]are crucial for generating comprehensive and detailed retinal imaging. The overall quality of the image is influenced not only by acquisition protocols but also by the exclusion of suboptimal scans and the rigor of preprocessing methods. Binary classification datasets commonly compare CSCR with normal controls (e.g., Hassan et al., 2021: CSCR = 306, Normal = 628). Multi-class approaches extend to CSCR subtypes, such as acute, chronic, or non-resolving (Yoon et al., 2022), and enable differential diagnosis among CSCR, AMD, CNV, DME, and drusen (He et al., 2023). Class imbalance remains a critical issue, as shown in Xu et al. (2021) [64] (serous retinal detachment (SRD, typically caused by SRF): 1,183 vs. non-SRD: 9,375) and Khan et al. (2023) (CSCR: 166 vs. Normal: 745). Persistent challenges include small sample sizes (e.g., Aoyama et al., 2021 with only 100 images), class imbalance, and variability in imaging protocols [28–30]. Distribution of the samples, illustrated in [Appendix B].

Task-Specific model performance

Binary classification

The objective of this section is distinguishing between CSCR vs. non-CSCR, SRD vs. non-SRD, and macula-off SRD vs. macula-on SRD.

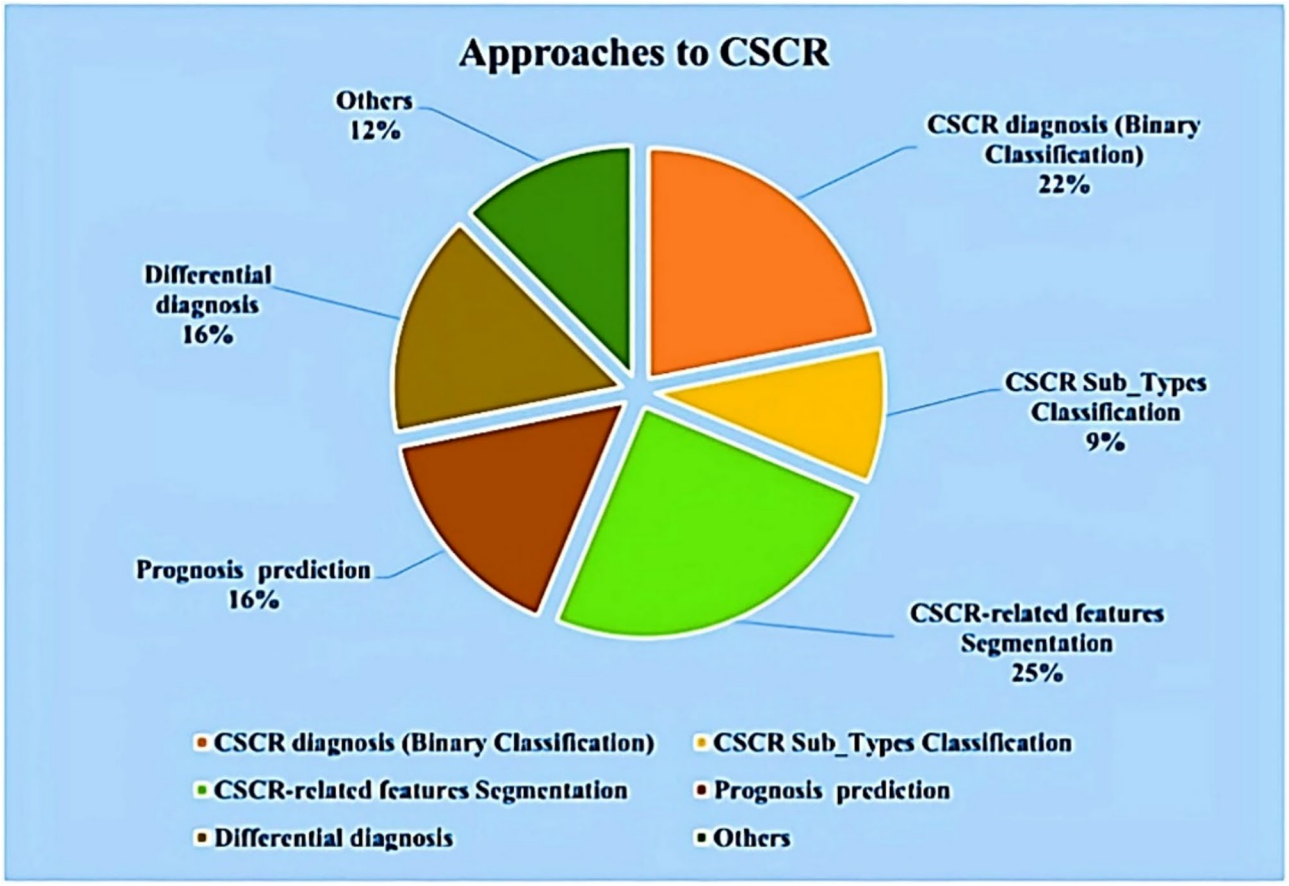

Fig. 3 Deep learning approaches to CSCR

Input modalities The reviewed studies use three types of input data: OCT (B-scan, En-face), CFP, and Blue-Wavelength Fundus Autofluorescence (BWFA) [65].

Common models Various deep learning strategies, primarily based on CNN architectures such as DenseNet, AlexNet, GoogleNet, and ResNet-18 are commonly used, as are multimodal fusion models like CA-Net [66]. Transfer learning with pre-trained networks (e.g., VGG-16, VGG-19, InceptionV3) [67] and custom CNN models built on platforms such as the Sony Neural Network Console (NNC) has also been reported. For SRD classification, approaches based on deep CNN architectures, such as EfficientNet-B0, have been utilized. EfficientNet-B0 offers a balance between model depth and complexity, thereby achieving high diagnostic accuracy. CA-Net uses lightweight designs, including: MobileNet to improve efficiency. The binary classification methods, along with their respective datasets and performance metrics, are detailed in Table 2.

Key observations OCT B-scans were the predominant imaging Modality. DenseNet demonstrated exceptional performance, achieving an accuracy of 99.78% for CSCR diagnosis on OCT images. Conversely, Models employing CFP demonstrate variability, with accuracies ranging from 85.7 to 94.6%. Furthermore, ResNet, when applied to OCT images, and VGG-19, when employed on BWFA images, have achieved accuracies that surpass 97% in binary classification. Notably, the Sony NNC-based model outperforms VGG-16 in CSCR detection. CA-Net, leveraging attention mechanisms and lightweight designs, demonstrated improved lesion detection; however, its performance was validated using datasets unrelated to CSCR (i.e., the COVID-19 X-ray dataset and the Lymphoma dataset). This underscores the importance of conducting external validation using CSCR-specific or ophthalmic datasets to ensure generalizability.

Performance evaluation metrics The most common evaluation metrics used in the reviewed studies are accuracy and AUC.

$$\text{Accuracy} = \frac{\text{TP} + \text{TN}}{\text{TP} + \text{TN} + \text{FP} + \text{FN}}$$

-.

Table 2 Comparative performance of deep learning models for CSCR detection

Study	Input	Task	Method	Dataset	Accuracy	Remarks
Hassan et al., 2021 [4]	OCT (B scan)	CSCR vs. Non-CSCR	AlexNet, GoogleNet, ResNet-18	Public dataset (OCTID) Total:500 (Macular Hole, AMD, CSCR, DR, Normal), 100 images per class	AlexNet: 99.6%; GoogleNet: 96.4%; ResNet-18: 98.2%	Pre-trained CNNs excel in binary tasks
Aoyama et al., 2021 [63]	OCT (En face)	CSCR vs. Non-CSCR	From scratch (Back-end_VGG16), Sony NNC + Grad-CAM	Clinical OCT dataset, Total: 100 (CSCR:53, Normal: 47)	VGG16: 88.0%; Sony NNC: 95.0%	The Sony platform has better performance.
Xu et al.,2021 [61]	CFP	SRD vs. Non-SRD	EfficientNet-B0	Total:10,558, SRD:1,183, non-SRD: 9,375. 1,183 SRD images to discern macula-off SRD from macula-on SRD	SRD/non-SRD: 0.920 Macula on/off: 0.852	Effective for macula-on/off SRD
Nelson et al.,2023 [65]	BWFA	CSCR vs. Non-CSCR	VGG-19	local eye hospital in Cochin, Kerala, India: Normal:1600, CSCR: 1608	97.3%	High accuracy with VGG-19
Zhou et al.,2020 [66]	CFP	CSCR vs. Non-CSCR	CA-Net (DenseNet + MobileNet)	In-house CFP dataset, Total: 556 (CSCR:409, Normal: 147)	94.6%	Attention to the patch containing the lesion to enhance discrimination.
Zhen et al.,2020 [67]	CFP	CSCR vs. Non-CSCR	InceptionV3 and 2 Inter-rater comparisons	Clinical CFP dataset, Total: 2504 (CSCR:1329, Normal:1175)	85.7%	Lower performance vs. OCT-based models
Hassan SA et al., 2023 [68]	OCT, CFP	CSCR vs. Non-CSCR	DenseNet, DarkNet	Clinical OCT dataset, Total 309 (CSCR:102, Normal:207) Clinical CFP dataset, Total: 52 (CSCR:14, Normal:38)	Accuracy: 99.78%, Sensitivity: 99.6%, Specificity:100%, F1 score: 99.52%	The proposed model is effective and efficient for CSCR detection using the OCT dataset.

- AUC: Plots True Positive Rate (TPR) vs. False Positive Rate (FPR) across thresholds.

While accuracy is often prioritized, sensitivity, specificity, and precision are crucial for clinical relevance. However, it is important to acknowledge that certain studies do not explicitly report these measures.

$$\text{Sensitivity} = \frac{\text{TP}}{\text{TP} + \text{FN}}$$

-

$$\text{Specificity} = \frac{\text{TN}}{\text{TN} + \text{FP}}$$

-

$$\text{Precision} = \frac{\text{TP}}{\text{TP} + \text{FP}}$$

-.

Another validation metric is fivefold Cross-Validation. This ensures robustness by partitioning the data into five subsets for iterative training/testing.

Multiclass classification

This section delineates the distinctions among non-CSCR, acute CSCR, and chronic CSCR. Chronic CSCR is further sub-classified into chronic atrophic, inactive, and non-resolving forms.

Input modalities The OCT (B-scan, 3D-OCT volumes) has been utilized for this task.

Common models A diverse set of architectures has been utilized for CSCR classification, including custom architectures (e.g., 13-layer CNNs), pre-trained networks such as VGG-16, ResNet-50, and Inception-V3, and multimodal fusion models. Additionally, modular classification pipelines [69] have been proposed, comprising the Single Image Prediction (SIP) and Final Decision (FD) modules. The SIP module typically employs ResNet-50 and VGG-19 for feature extraction from individual images, while the FD module integrates logistic regression, support vector machines (SVMs), and XGBoost to aggregate predictions and enhance overall classification accuracy. This modular approach leverages both deep learning and traditional machine learning techniques to improve robustness and interpretability.

The methods used for CSCR subtype differentiation, along with their corresponding datasets and performance metrics, are detailed in Table 3.

Key observations Large datasets, such as the one from Hangil Eye Hospital (7,425 images), have been shown to enable high subtype accuracy. Custom CNN architectures (accuracy: 97%) outperform pre-trained CNN models. The SIP-FD modular pipeline improves subtype classification accuracy by leveraging deep learning models for initial predictions (ResNet50) and statistical classifiers (Logistic Regression) for final decision-making (accuracy: 94.2%).

Table 3 Comparative performance of deep learning models for subtype differentiation

Study	Input	Task	Method	Dataset	Accuracy
Yoon et al.,2020 [41]	OCT (B scan)	CSCR vs. Non-CSCR, and Non-CSCR vs. Acute-CSCR vs. Chronic-CSCR	CNN from scratch (13 CNN layers + ReLU + 4 max pooling layers + 2 dropout layers + 4 FC Layers + softmax) + Grad-CAM	Hangil Eye Hospital, Total: 2360, Normal: 900, CSCR: 1460 (acute:466, Chronic: 994)	Binary: 93.8%, Sub-Type: 97.6%
Hwang et al.,2022 [69]	OCT (B scan), 3D-OCT	Acute-CSCR vs. Chronic-CSCR vs. Normal	Two different modules: SIP (Single Image Prediction) and FD (Final Decision), SIP: ResNet-50, VGG19, FD: Logistic regression, SVM, XGB, Model: (ResNet-50 + Logistic regression, VGG19 + Logistic Regression, VGG19 + SVM, VGG19 + XGB), CNN-LSTM, 3D-CNN (25 SD-OCT)) + 1 to fivefold cross validation + Transfer Learning	Hangil Eye Hospital Total: 7425, (acute CSCR: 2725, Chronic CSCR: 2650, Normal: 2050), 3D-OCT: 25 Volume.	ResNet-50 + Logistic Regression: 94.2%, VGG19 + Logistic Regression: 92%, VGG19 + SVM: 90%, VGG19 + XGB: 89%, CNN-LSTM: 83%, 3D-CNN: 75.6%
Yoon et al.,2022 [44]	OCT (B scan)	Active-CSCR vs. Non-resolving CSCR vs. Chronic-CSCR vs. Inactive-CSCR	CNN-Based Models (VGG-16, ResNet-50, Inception-V3) + fivefold cross validation	Clinical OCT datasets Total: 3874, (Acute: 1090, Non-resolving: 1084, Chronic: 898, Inactive: 802)	VGG-16: 70.0%; ResNet-50: 68.6%; Inception-V3: 68.2%

Performance evaluation metrics It has been demonstrated that Performance Evaluation Metrics are analogous to binary classification.

Segmentation

Segmentation involves precisely delineating certain lesions (e.g., SRF, PED, and RPE atrophy) in retinal images.

Input modalities The segmentation methods reviewed primarily deal with two types of imaging modality: FFA images [26] and OCT B-scans and volumes [36, 52]de Moura et al., 2021; Narendra Rao et al., 2019].

Common models Deep learning techniques have been widely used to identify and segment clinically relevant features, including leakage points, the optic disc (OD), and the macula in FFA images, as well as SRF in OCT images. Attention Gate Networks (AGN) use attention mechanisms to improve the localization of leakage points in FFA images. Capsule network variants with dynamic routing between capsules have been shown to improve OCT-based SRF segmentation by preserving spatial relationships. Encoder–decoder architectures with skip connections, such as Feature Pyramid Networks (FPN), fully convolutional networks (FCNs) based on U-Net, and U-Net derivatives, are commonly used for SRF segmentation. In addition, the SegNet architecture [70] has been adopted in FCN-based segmentation [71] frameworks to enable fully convolutional processing for fluid delineation.

The key segmentation methods, along with their associated datasets and performance metrics for the studies discussed in this section, are summarized in Table 4.

Key observations Most studies have focused on segmenting SRF, with OCT B-scans as the primary input modality. U-Net variants are commonly used for OCT-based segmentation tasks. Capsule networks and attention mechanisms have been introduced to enhance segmentation precision. For leakage point segmentation on FFA, attention-gated networks (AGN) achieved the highest Dice coefficient of 0.949. FCNs based on SegNet have reported Dice scores up to 0.965 for SRF segmentation. Capsule networks have improved spatial accuracy, especially for small lesions. Recent advancements in few-shot learning have led to significant progress in retinal vessel segmentation and reduced reliance on large annotated datasets. These methods utilize multi-scale feature extraction, feature fusion, and attention mechanisms to enhance segmentation performance and cross-domain adaptability, which is essential for clinical datasets with heterogeneous distributions.

Table 4 Comparative performance of deep learning models for segmentation

Study	Input	Task	Method	Dataset	Performance Metrics
Chen et al.,2021 [19]	FFA Images	AGN: leakage points segmentation, U-Net (Optic Disk segmentation, U-Net (macula segmentation)	AGN (Attention-gated network) for segmenting leakage points, U-net for segmenting the optic disk (OD), and the macula region	Hospital of Zhejiang University Total: 2108 FFA Images. 1229 images for training, 439 images for validation, and 440 for test	AGN (leakage points): 0.949; U-Net (OD): 0.850; U-Net (macula): 0.920
Gende et al.,2024 [43]	OCT B-scans	SRF segmentation	FPN (Feature Pyramid Network) with various encoders (MobileNet, DenseNet, ResNet), U-Net with various encoders (MobileNet, DenseNet, ResNet)	Total: 100 OCT B-scans, CSCR:85, Normal: 15	FPN + MobileNet: 0.853; FPN + DenseNet: 0.861; FPN + ResNet: 0.849; U-Net + MobileNet: 0.837; U-Net + DenseNet: 0.859; U-Net + ResNet: 0.868
Pawan et al.,2021 [59]	OCT B-scans	SRF segmentation	SegCaps, DRIP-Caps (CapsuleNet enhancement), and U-Net	Total: 25 volumetric OCT (Each volume has 128 B-scans)	SegCaps: 0.9424; DRIP-Caps: 0.9404; U-Net: 0.9281
de Moura et al.,2021 [70]	OCT B-scans	SRF segmentation	FCN (Fully Convolutional Network) based on SegNet,	Total: 100 OCT B-scans, CSCR:85, Normal: 15	Global Dice coefficient: 0.965
Xu J et al., 2022 [72]	Retinal vessel images	Retinal vessel Segmentation with minimal samples	Few-Shot Learning	public datasets (DRIVE, CHASE_DB, STARE) and a private CSCR clinical dataset	AUC on DRIVE: 98.3%, AUC on CSCR data: 97%
Narendra Rao et al., 2019 [71]	OCT B-scans	SRF segmentation	FCN-based U-Net	Pink City Eye and Retina Center, Jaipur, India: 15 OCT volumes (1920 B-scans)	Dice: 0.910, Recall: 89.0%, Precision: 93.6%

Performance evaluation metrics The studies reviewed primarily used the Dice Similarity Coefficient (DSC) to evaluate segmentation performance.

$$\text{Dice} = \frac{2\times \mid \text{X} \cap \text{Y} \mid}{\mid \text{X} \mid + \mid \text{Y} \mid}$$

-.

Another validation metric is Intersection over Union (IoU), which measures the overlap between the predicted and true segmentation area relative to each other.

$$\text{IoU} = \frac{\text{TP}}{\text{TP} + \text{FP} + \text{FN}}$$

-.

Segmentation with classification

The objective of this section is twofold: first, to perform segmentation for delineating SRF, followed by classification to diagnose CSCR.

Input modalities Contribution employs the CFP for SRF segmentation [62].

Common models The segmentation of SRF in CFP images has been addressed using deep learning models like GAN-based frameworks (Pix2Pix), U-Net, Conditional GAN (PatchGAN), and FCN-8s. The Pix2Pix model integrates U-Net and PatchGAN to improve feature representation through adversarial learning. Additionally, InceptionV3 has been employed for classifying CSCR versus normal CFP images. FCN-8s, leverages deep convolutional layers for pixel-wise segmentation. These methodologies predominantly utilize encoder–decoder architectures with skip connections and, in GAN-based models, incorporate adversarial training to enhance segmentation accuracy.

The segmentation-with-classification methods, covering model architectures, datasets, and performance metrics such as Dice score and accuracy, are summarized in Table 5.

Key observations As reported by Yoo et al. (2022), the segmentation performance was Moderate, with a Dice similarity coefficient of 0.763. In contrast, the classification model based on InceptionV3 exhibited high diagnostic accuracy (97.0%) and an AUC of 0.989, thereby substantiating its efficacy in differentiating CSCR from normal cases. However, segmentation-specific metrics, such as sensitivity (70.2%), were comparatively lower, suggesting that segmentation quality may influence the reliability of downstream classification tasks. These findings underscore the necessity to strike a balance between the precision of segmentation and the accuracy of classification.

Performance evaluation metrics It has been demonstrated that the performance evaluation metrics of this approach are combinations of metrics used for segmentation and binary classification.

Table 5 Performance of deep learning models for segmentation with binary classification to diagnose CSCR

Study	Input	Task	Method	Dataset	Performance Metrics
Yoo et al., 2022 [62]	CFP	SRF Segmentation, CSCR Classification	Segmentation: Pix2pix (U-Net + PatchGAN), FCN-8s, Classification: InceptionV3	194 CFPs of SRF lesions (Aerospace Medical Center) + 98 CFPs (public RFMiD dataset), Binary Classification: (98 CSCR + 9 Normal)	U-Net based on pix2pix (Dice: 0.763, IoU: 0.619, Sensitivity: 70.2%, Specificity: 98.8%, Precision: 86.2%), FCN-8s (Dice: 0.726, IoU: 0.582, Sensitivity: 70.6%, Specificity: 97.8%, Precision: 82.4%) Binary Classification (Accuracy: 97.0%, AUC: 0.989, Sensitivity: 95.5%, Specificity: 100%)

Differential diagnosis

The objective of this section is to differentiate CSCR from other retinal disorders and detect complications such as CNV. CSCR shares imaging features with AMD [73] PCV, DME [74]– [75]Vogt-Koyanagi-Harada (VKH), and uveitis. CNV, characterized by abnormal proliferation of choroidal vessels, can lead to visual disturbances similar to those observed in CSCR, particularly in chronic forms where secondary CNV may develop [76]. Other conditions with overlapping characteristics include ischemic optic neuropathy (ION), optic neuritis (ON), and ocular tumors such as choroidal melanoma and metastatic lesions [77–79]. These similarities complicate the diagnostic process, especially in atypical and chronic cases. Therefore, the timely detection of complications such as CNV is imperative for accurate diagnosis and appropriate management. This section explores the role of deep learning models in addressing these diagnostic challenges and explores the potential of advanced methods for enhancing differential diagnosis.

Shared imaging features and diagnostic challenges OCT findings, including PEDs and SRF, are commonly associated with CSCR, AMD, and PCV. The presence of drusen and neovascular membranes in AMD often overlaps with CNV seen in chronic CSCR. For precise differentiation, multimodal analysis using patterns like the "smoke stack" sign in FAF for CSCR and drusen deposits in AMD is recommended [34, 35, 40]. Data from FFA and ICGA are valuable for distinguishing these retinal disorders. Although fluid accumulation in DME can resemble CSCR, DME demonstrates specific vascular alterations such as capillary dropout and microaneurysms, which deep learning algorithms can detect. VKH disease and uveitis may both present with SRF and inflammation. VKH is typically characterized by bilateral choroidal thickening, whereas uveitis can be identified by the presence of inflammatory biomarkers detectable using artificial intelligence (AI)-based methods.

Input modalities Researchers employ FFA and OCT imaging to differentiate CSCR from AMD, DME, and other retinal diseases.

Common models In CFP-based differential diagnosis [80]pre-trained CNN architectures such as ShuffleNet-V2, ResNet, DenseNet, and MobileNet are utilized to extract retinal features for distinguishing CSCR from other retinal conditions. Vision Transformer models, including the Conditional Transformer (C-Tran), use masked label training (MLT) to enhance multi-label learning performance. Rodríguez et al. [81] implemented a framework that combines DenseNet-161 for feature extraction with C-Tran for multi-label learning. ResNet-50, InceptionV3, and DenseNet-201 demonstrate high proficiency in extracting features from OCT images. Ant Colony Optimization (ACO) algorithms further improve feature selection on OCT images, resulting in increased classification accuracy. The Swin-Poly Transformer model generates interpretable predictions for retinal diseases by making feature-based decisions on OCT images.

A comparison of differential diagnosis performance across imaging modalities, highlighting each method, its dataset, and key diagnostic metrics such as accuracy and AUC, is presented in Table 6.

Key observations The first fundus image dataset created with a balanced class distribution and strict quality control procedures is the MuReD dataset. OCT-based models show better diagnostic performance (AUC: 0.999) than CFP-based models, which have trouble differentiating between several retinal disease classes. This is probably because OCT imaging offers a higher structural resolution. On OCT-based multi-class classification tasks, Transformer-based models (such as Swin-Poly) and

Table 6 Comparative performance of deep learning models for differential diagnosis of CSCR

Study	Input	Task	Method	Dataset	Performance Metrics	Differential Diagnosis
Khan et al.,2023 [42]	OCT	Multi-Class Classification	Feature Extraction (ResNet-50, InceptionV3, DenseNet-201) ± Feature selection (Ant Colony Optimization (ACO)) + Classification (KNN and SVM)	Soonchunhyang University Bucheon Hospital, Total: 2998	DenseNet-201 + ACO (Accuracy: 99.1%, AUC: 1.000, Precision: 98.9%, Recall: 98.2%, F1-score: 98.5%).	CSCR vs. AMD, BRVO, CRVO, DME
He J, et al.,2023 [48]	OCT	Multi-Class Classification	Interpretable Swin-Poly Transformer	OCT2017 (Kermany, D. S. et al.):109,312, OCT-C8 (Subramanian, et al.): 24,000	Accuracy: 99.8%, AUC: 0.999, Precision: 99.8%, Recall: 99.8%, F1-score: 99.8%.	CSCR vs. AMD, CNV, DME, MH, DR, drusen, and Normal
Wen et al.,2020 [80]	CFP	Normal vs. Abnormal, and CSCR vs. CECR	Part of ShuffleNet-V2 (first three stage of Pretrained ShuffleNet-V2) compared to InceptionV3, ResNet-18, DenseNet-121, MobileNet-V2.	Sichuan Provincial People's Hospital, Total: 718 (Normal: 240, CSCR: 409, CECR: 69)	ShuffleNet-V2: Accuracy: 97.7%, Precision: 99.6%, Recall: 98.9%, F1-score: 99.2%.	CSCR vs. Central Exudative Chorioretinopathy (CECR)
Rodríguez et al.,2023 [81]	CFP	Multi-Class Classification Based on Vision Transformer	Vision Transformer-based model with DenseNet161 backbone + masked label training (MLT) to learn label correlations.	MuReD is constructed using a number of publicly available datasets. Total: 2,797	AUC: 0.962, Precision: 68.5%, Recall: 49.2%, F1-score: 57.3%.	20 disease labels (e.g., DR, ARMD, CSCR) + "NORMAL" and "OTHER"

hybrid frameworks that combined DenseNet-201 with Ant Colony Optimization (ACO) outperformed the other evaluated architectures (accuracy: 99.1%, AUC: 1.000). On the other hand, lightweight CNNs, like ShuffleNet-V2, performed best for binary classification based on CFP (accuracy: 97.7%). These findings demonstrate the growing significance of Transformer architectures as workable substitutes for the diagnosis of multi-class retinal diseases.

Performance evaluation metrics ShuffleNet-V2 reports F1 scores up to 0.992 for binary classification. For multiclass tasks, AUC and Mean Average Precision (MAP) were emphasized for robustness.

AUC and MAP were used to address class imbalance in multi-disease datasets.

$$\mathrm{F1-score} = \frac{2 \times \mathrm{Precision} \times \mathrm{Recall}}{\mathrm{Precision} + \mathrm{Recall}}$$

-.

- MAP = Average precision across all classes.

Prognosis

In addition to diagnosis, forecasting the clinical trajectory and therapeutic response is essential. This job includes predicting when a disease will come back, figuring out how well treatment works, and keeping an eye on long-term progress.

Input modalities The combination of CFP and clinical data is used to guess how well SRF will be absorbed after PDT. Simultaneously, OCT-based methods (B-scan and en face) are employed to evaluate the persistence of CSCR after a 6-month interval and the response to PDT in chronic CSCR after 3 months.

Common models The CSCR prognosis comes from a fusion model (DeepPDT-Net) [82] that combines ResNet-50 and XGBoost. This integration makes it easier to guess what will happen to the SRF after PDT. Using SHAP and Grad-CAM techniques to validate clinical decisions makes the model easier to understand. To predict SRF persistence using OCT, ResNet-50 is used to get features from images of the retinal thickness, mid-retina, ellipsoid zone, and choroidal layers. Layer-Specific Image Analysis helps find out how a disease is getting worse. Moreover, Grad-CAM activation maps are employed to emphasize the critical features that facilitate persistence. The prediction of the PDT response on OCT images used a DenseNet model [83] that can classify groups and tell the difference between complete, partial, and absent SRF resorption.

The prognostic performance metrics for CSCR are detailed in Table 7.

Key observations DeepPDT-Net combining ResNet-50 with XGBoost, exhibited superior performance in comparison to standalone Models, achieving an accuracy of 86.4% and an AUC of 0.917 during external validation by leveraging both imaging and clinical data. Research indicates that integrating OCT-derived features, such as B-scans and retinal thickness Measurements, provides the Most reliable approach for predicting CSCR persistence, yielding an accuracy of 95.2% and specificity of 97.62%. Additionally, layer-specific analysis of OCT parameters, including retinal thickness and the ellipsoid zone, has been shown to improve prognostic precision.

Table 7 Comparative performance of deep learning models for prognosis predicting and treatment response of CSCR

Study	Input	Task Type	Method	Dataset	Performance Metrics
Jee et al.,2022 [44]	OCT (B-scan and en face)	Predict CSCR persistent after 6 months using OCT of retinal thickness (RT), mid-retina, ellipsoid zone (EZ) layer, and choroidal layer	ResNet50 + Grad-CAM	Vincent Hospital, Total: 832 (self-resolving:593, persistent:239)	Accuracy: (B-scan: 80.72%, RT: 92.0%, Mid-retina: 64.8%, EZ: 92.0%, Choroid: 63.2%). F1-score: (B-scan: 68.0%, RT: 87.18%, Mid-retina: 31.25%, EZ: 87.18%, Choroid: 11.54%). Specificity: (B-scan: 89.29%, RT: 96.43%, Mid-retina: 84.52%, EZ: 96.43%, Choroid: 90.48%). (B-scan + RT)-Accuracy: 95.20%, F1-score: 92.50%, Specificity: 97.62%; (B-scan + EZ)-Accuracy: 88.00%, F1-score: 81.01%, Specificity: 92.86%; (EZ + RT)-Accuracy: 92.80%, F1-score: 89.16%, Specificity: 94.05%;
Yoo et al.,2022 [62]	multimodal (CFPs and Clinical data)	Predict SRF absorption post-PDT (after 1 year).	DeepPDT-Net (ResNet-50 + XGBoost)	Severance Eye Hospital, (147 target CFP) + Gangnam Severance Hospital (19 target CFP) Total: 911 (target: 166, Normal: 745), Clinical data (sex, age, Anti-VEGF)	predicted treatable and refractory CSCR-ResNet50 (Accuracy: 83%, AUC: 0.839, Sensitivity:67.7%, Specificity:87.1%) XGBoost (Accuracy:72.1%, AUC: 0.784, Sensitivity:77.4%, Specificity: 70.7%), DeepPDT-Net (Accuracy: 86.4%, AUC: 0.880, AUC for External Validation: 0.917, Sensitivity:74.2%, Specificity: 89.7%)
Fernández-Vigo et al.,2022 [83]	SD-OCT	prediction of the response to PDT in chronic CSCR after 3 months: Group 1, complete SRF resorption, Group 2, partial SRF resorption, Group 3, absence of any SRF resorption.	DenseNet	Total: 216 (CSCR + SRF persistent), Group1: 100, Group2: 66, Group3: 50.	Accuracy: Compares all groups (Group1, Group2, and Group3): 0.53 compares groups 1 vs. 2: 0.67 compares groups 2 vs. 3: 0.68

Despite these advances, group comparison scores (e.g., 0.68) underscore the persistent difficulty in distinguishing partial from complete SRF absorption following PDT. CNNs have been utilized not only to predict persistence but also to forecast treatment response, estimate post-treatment visual acuity, and evaluate macular involvement by extracting CSCR-related choroidal patterns [84]– [85].

Performance evaluation metrics For the prediction of treatment outcomes (e.g., SRF absorption after PDT), accuracy, AUC, sensitivity (recall), and specificity have been used. For prediction of disease persistence (e.g., chronic CSCR), accuracy, F1 score, specificity, and layer-specific performance, and for prediction of therapeutic response (e.g., PDT efficacy), the group comparison score is reported. It is an accuracy or statistical score for differentiating treatment response groups (complete, partial, no SRF absorption).

Discussion

The systematic evaluation of deep learning approaches for CSCR diagnosis underscores their transformative potential in addressing the limitations of conventional diagnostic methods.

Model architectures

Deep learning architectures, particularly CNN-based Models such as ResNet, VGG, and DenseNet, have demonstrated high diagnostic accuracy. OCT-based Models consistently outperform CFP-based models due to superior structural detail and visualization of the SRF and the PED. For instance, DenseNet achieved 99.78% accuracy in binary classification using OCT, compared with 85.7–94.6% for CFP models (Table 2). CNNs, while effective for feature extraction, present challenges in interpretability [73]; methods such as Grad-CAM and SHAP provide partial insights but fail to fully capture decision-making. Custom CNN models tailored for CSCR have outperformed pretrained architectures and, in some metrics, even ophthalmologists [86]. Vision Transformers (ViTs), leveraging self-attention to model long-range dependencies [37]offer promising interpretability and competitive performance (e.g., Swin-Poly, AUC: 0.999) but require larger datasets. Despite the fact that these advanced architectures have not yet been widely applied for CSCR diagnosis, there is considerable potential for enhancing accuracy and robustness, warranting further investigation [48, 81, 87]– [88]. Segmentation tasks are dominated by U-Net variants, with attention-gated and capsule networks (e.g., SegCaps) improving accuracy

(Dice coefficient range: 0.949–0.965; see Table 4). Deep learning is proven to localize and quantify features like SRF and PED, so future models will extend this to other markers like vascular abnormalities, choroidal hyperpermeability, and RPE integrity changes [16, 89]. Despite these advances, dataset development remains resource-intensive due to reliance on expert annotation Semi-automated labeling and crowdsourcing approaches may mitigate this burden. While the efficacy of Subtype classification models is evident, they encounter challenges in distinguishing between acute and chronic subtypes due to the overlap in imaging features. However, modular pipeline models (e.g., SIP-FD, accuracy: 94.2%) show promise. Prognostic models, particularly DeepPDT-Net (86.4% accuracy; see Table 7), underscore the value of integrating imaging with clinical data for predicting treatment responses. However, distinguishing between partial and absent SRF resorption remains a formidable challenge.

Multimodal imaging

The integration of multimodal imaging (e.g., OCT, FFA, ICGA, FAF) enhances diagnostic capability by combining complementary data sources, improving lesion detection, vascular assessment, and evaluation of Choroidal hyperpermeability. Incorporating ICGA and FFA has been shown to increase chronic CSCR detection accuracy by up to 12% [12], while aiding leakage-point localization and differentiation from PCV and AMD [32, 40]. ICGA's ability to identify choroidal hyperpermeability further supports its role in distinguishing CSCR from polypoidal lesions [22]. Such models demonstrate superior performance across machine-learning tasks by leveraging diverse data sources [42, 90]. Multimodal fusion models, which integrate multiple imaging modalities and clinical parameters (e.g., demographics, history, laboratory data, genetic markers), outperform single-modality CNNs and allow individualized decision-making [56, 88, 91]. Emerging approaches, such as registering FAF with OCT, have improved early detection and characterization of subtle structural changes [90]. Overall, multimodal fusion is expected to facilitate earlier and more accurate CSCR diagnosis, guide tailored treatment strategies, and enhance prognostic prediction. A schematic example of a multimodal fusion framework is shown in Fig. 4.

Preprocessing pipelines

Real-world ophthalmic images often contain noise and artifacts resulting from patient movement or device limitations. Preprocessing steps, including standardization, normalization, and region-of-interest cropping, are essential for improving model performance; however, robustness to such variations must also be integrated into model design [42, 46, 50]. Diagnostic speed depends on dataset size, heterogeneity, and algorithm optimization [17]. While Moderate datasets achieve high accuracy for binary classification, Multiclass tasks, such as differentiating acute, non-resolving, chronic, and inactive stages, remain challenging, with reported accuracies ranging from 68 to 70%. Emerging approaches, including few-shot learning, domain adaptation, and synthetic data generation via GANs or diffusion models [67, 92]may mitigate data scarcity. For multimodal integration, standardized preprocessing pipelines addressing noise, alignment, and normalization are required to enhance data quality and ensure interoperability, thereby improving diagnostic accuracy and robustness.

Emerging trends, Few-Shot learning and advanced data augmentation

Presently, publicly accessible datasets tailored for CSCR diagnosis are limited, which restricts the performance of traditional deep learning models [4, 20]. To overcome these limitations, several strategies have been suggested, such as transfer learning, domain adaptation, and synthetic data generation. Recent developments in Few-Shot Learning (FSL), Generative Adversarial Networks (GANs), and diffusion models have shown great promise in alleviating data scarcity and improving diagnostic precision [21, 66]– [67]. For instance, a study investigated the combination of FSL and GANs for enhancing the detection of rare retinal diseases using OCT, with a diagnostic accuracy of 92.1% on an experimental dataset, a level of performance comparable to expert ophthalmologists. This strategy highlights the value of advanced techniques in overcoming dataset restrictions that limit the effectiveness of traditional deep learning methods.

- Few-shot learning (FSL): FSL is a model training method with little labeled data. The objective of these techniques is to generalize over tasks with few examples. This goal is achieved using learning paradigms that learn transferable features or leverage prior knowledge. For instance, Xu J. et al. [72] have presented a few-shot learning method for robust retinal vessel segmentation with few samples. Retinal vessel segmentation is crucial for laser surgery on CSCR to avoid vessel rupture and improve surgical accuracy. The Few-Shot Adaptation method formulates retinal vessel segmentation as a few-shot problem by considering each patient's retinal image as an individual "class." The patches from these images are then used to create support sets for training and query sets for testing. The method employs episodic training with CC-way KK-shot learning (e.g., 5-way 3-shot) to mimic the paucity of real-world data. The baseline model is built upon the base of VGG16's encoder, extended

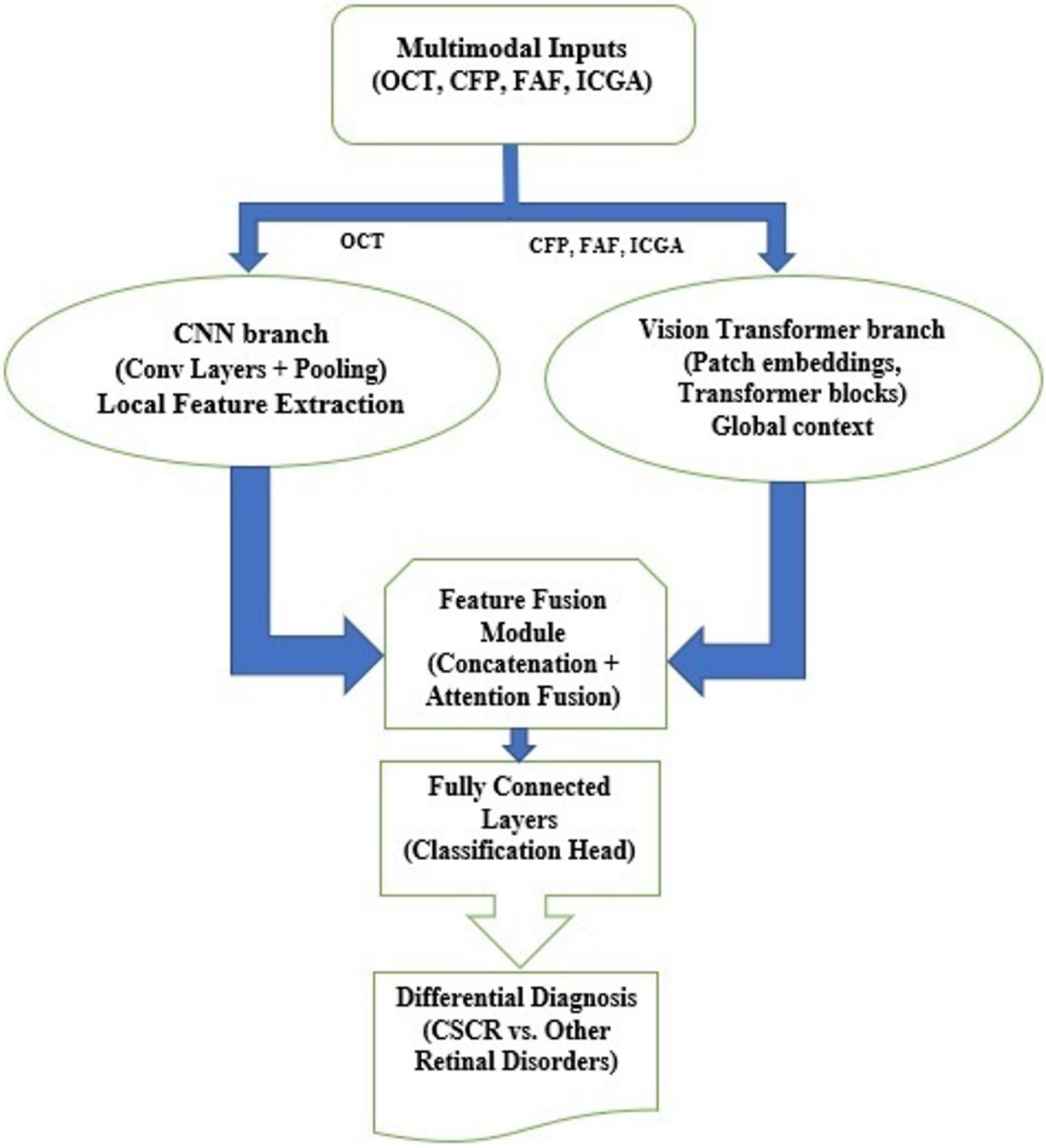

Fig. 4 Multimodal fusion model

with Mask average pooling to allow the extraction of class prototypes. Multi-scale class prototypes have been employed to extract vessel features at varied resolutions. Integration of multi-scale information is done through feature fusion using skip connections. Multi-scale attention modules have been used to make use of global context for improved vessel localization. Meta-learning, a variant of FSL, has reached an accuracy of 85% with 50 samples, alleviating data scarcity [20].

- Diffusion method: Diffusion models represent a subcategory of generative artificial intelligence that has been developed to generate high-quality images through the process of denoising random noise into structured data [42]. Diffusion models differ from GANs by employing a forward (noise addition) and reverse (denoising) process to generate realistic

images. They've successfully generated synthetic OCTs that are hard to tell apart from real ones. These models can help balance class data (e.g., acute vs. chronic CSCR) for classification, and provide annotated data (e.g., SRF masks) for improving segmentation networks like U-Net and CapsuleNet. They can also create OCT, FFA, and ICGA pairs for more advanced multimodal learning. Diffusion models outperform GANs in terms of image sharpness and realism. Conditional diffusion models can generate disease-specific variations, like different SRF volumes.

Clinical translation and recommendations

Deep learning models, particularly those based on high-resolution OCT, have the potential to significantly improve how CSCR is managed. Automated OCT analysis can detect early or subtle cases, helping non-specialist clinics identify patients who need prompt referral. Segmentation networks can generate probability maps that distinguish CSCR from AMD, PCV, and DME, reducing misdiagnoses. Tracking SRF and PED volumes over time provides objective measures of treatment response, guiding decisions about photodynamic therapy (PDT), steroid management, or closer follow-up. When combined with clinical information, such as age, corticosteroid use, and symptom duration, multimodal models can predict recurrence risk and help tailor personalized follow-up schedules. To make these models clinically useful, standardized evaluation is crucial. Metrics should include:

- Screening: Automated OCT analysis can detect early or subclinical CSCR, helping non-specialist clinics identify patients who need prompt referral. Performance should be assessed using metrics such as sensitivity, negative predictive value (NPV), AUROC, and F1-score.
- Differential diagnosis: Probability maps from segmentation networks can reliably distinguish CSCR from AMD, PCV, and DME, reducing misdiagnoses and inappropriate treatments. Evaluation metrics should include specificity, positive predictive value (PPV), and AUROC.
- Progression monitoring: Quantitative tracking of SRF and PED on serial OCT scans provides objective biomarkers to guide treatment decisions, including PDT timing or steroid tapering. Segmentation performance should be reported using the Dice coefficient, Jaccard index, and volumetric error.
- Prognosis and personalized care: Multimodal fusion models that combine imaging data with clinical variables (e.g., corticosteroid use, symptom duration, comorbidities) can predict fluid persistence or recurrence, enabling tailored follow-up and therapy. Prognostic performance should be assessed with AUROC, calibration metrics, and clinically relevant outcomes.

To ensure real-world utility, studies must include external validation with confidence intervals, follow reporting standards such as STARD-AI or CONSORT-AI, and provide clear documentation of preprocessing steps, hyperparameters, dataset demographics, and validation protocols. Prospective "silent trials" across multiple centers are recommended before widespread clinical implementation.

Seamless integration into clinical workflows is essential. Models should connect smoothly with Picture Archiving and Communication Systems (PACS) and Electronic Health Records (EHRs), support DICOM/HL7/FHIR standards, and feature user-friendly interfaces to reduce alert fatigue. Vision Transformers and attention-based architectures can enhance interpretability [87, 88]while combining imaging with clinical data helps identify patients at high risk of CSCR recurrence.

Interpretability remains a priority. Attention-based models, Grad-CAM, SHAP, and visual question answering can help clinicians understand AI decision-making.

Reported measures such as the Dice coefficient and AUC, frequently have no task-specific clinical thresholds, thereby reducing translational relevance. For instance, segmentation accuracy must meet clinically meaningful thresholds (See Table 8 for proposed benchmarks), ensuring that measurements of SRF or PED are precise enough to reliably guide treatment decisions, such as initiating or adjusting PDT. Table 8 is a suggestion and the

Table 8 Proposed performance benchmarks for the clinical deployment of deep learning models in CSCR management

Clinical Task	Metric	Proposed Minimum Threshold for Clinical Use	Rationale
Screening	Sensitivity	≥ 95%	To minimize false negatives and ensure all potential cases are referred.
Differential Diagnosis	Specificity	≥ 90%	To minimize false positives and avoid misdiagnosis/mistreatment.
SRF Segmentation	Dice	≥ 0.85	To ensure volumetric measurements are sufficiently accurate to track changes.
Prognosis	AUC	≥ 0.80	To demonstrate model utility in predicting outcomes better than chance.

Table 9 Domain-wise risk of bias assessment for 96 studies using adapted QUADAS-2 criteria

QUADAS-2 Domain	Low Risk	High Risk	Unclear	Key Findings
Patient Selection	24 (25%)	62 (65%)	10 (10%)	Asian-only cohorts (60%); excluded chronic CSCR
Index Test	43 (45%)	34 (35%)	19 (20%)	7% validation unreported; 35% preprocessing omissions
Reference Standard	58 (60%)	24 (25%)	14 (15%)	21 studies used a single annotator
Flow/Timing	29 (30%)	38 (40%)	29 (30%)	Class imbalance unaddressed in 62%
Reproducibility	17 (18%)	79 (82%)	0 (0%)	73 studies shared neither code nor data

thresholds would be refined based on a deeper literature review and clinician consultation.

Furthermore, sensitivity and specificity, particularly for atypical or chronic CSCR, are underreported. Future studies should evaluate AI models using clinically relevant metrics and stratified analyses, ensuring performance is reliable across disease stages, subtypes, and patient subgroups critical for real-world decision-making.

Finally, regulatory and ethical considerations, including patient privacy, data security, fairness, and bias mitigation, must be addressed. Federated learning provides a framework for multi-center training that preserves privacy under HIPAA/GDPR, while maintaining diverse datasets. By integrating rigorous evaluation, standardized reporting, and ethical safeguards, these approaches can bridge the gap between algorithmic innovation and safe, effective clinical deployment of AI-driven CSCR tools.

Critical discussion

Methodological limitations and risk of bias

This systematic review highlights both the remarkable progress and the persistent limitations in deep learning–based CSCR diagnosis. Although OCT-based CNNs and emerging transformer architectures consistently report high internal accuracy, several methodological, dataset, and reporting deficiencies hinder real-world applicability. Key limitations include dataset representativeness, validation rigor, and reproducibility. Geographic and modality biases, coupled with small or homogeneous cohorts, constrain generalizability. Furthermore, suboptimal validation strategies, inconsistent ground truth annotations, and limited code/data availability undermine transparency and impede independent verification. The following subsections detail these shortcomings and outline priority research directions for achieving clinically relevant and globally deployable AI solutions for CSCR. The risk-of-bias assessments for all 96 studies are summarized in Table 9, classified using the QUADAS-2 tool (see Sect. 2.5).

Dataset limitations, representativeness and modality bias

The majority of studies (65%) used OCT datasets alone. Although OCT is useful for SRF and PED detection, it cannot document all aspects of the disease. Multimodal imaging (FFA for active leakage points and ICGA for choroidal hyperpermeability) is crucial for differential diagnosis, stratifying severity, and for the detection of macular neovascularization in chronic or complicated cases [93–95]. For instance, hyperfluorescent plaques, not present on OCT, were noted in 72% of recurrent CSCR [94]and OCT alone may frequently be unable to differentiate between acute and chronic types [68]. A strong geographic bias exacerbates these shortcomings: More than 60% of datasets were from Asian populations, mainly Korean and Indian, with little representation of other populations. Such OCT-centered and geographically homogeneous sourcing threatens to overestimate reported performance and restricts generalizability to environments where multimodal imaging is the norm. Redressing these gaps necessitates large, demographically diverse, multimodal datasets garnered via international, multicenter collaborations with harmonized acquisition protocols and annotation standards. In addition, dependence on small, single-center, or proprietary cohorts incurs sampling bias, distorting class distributions and under-representing device variation. Acute CSCR predominated the datasets (≈70%), with chronic or treatment-resistant subtypes sparsely represented. Prospective, multicenter datasets with heterogeneous demographics (age, gender, ethnicity, disease severity) and images from dissimilar imaging platforms under vendor-agnostic quality controls are essential to provide assurance of robustness and clinical relevance of AI-powered CSCR tools.

Model development and validation

Transparency and reproducibility remain major concerns in current CSCR deep learning studies. Many studies, over one-third, did not report key preprocessing steps, such as normalization or artifact removal, making it difficult for others to replicate their findings. Validation strategies were often suboptimal: nearly a third of studies relied on non-independent test sets or omitted details on cross-validation, which increases the risk of data leakage. Although more than half employed k-fold cross-validation, only a small fraction (12%) performed external validation, limiting confidence in how well these models would perform in real-world settings.

Reference standard variability

The reliability of ground truth labels remains a concern, with approximately 20% of studies depending on a single annotator for tasks such as SRF boundary delineation. Inconsistent labeling protocols further limit the comparability across studies, particularly for tasks requiring high precision. Employing multi-grader consensus and standardized annotation guidelines is imperative to reduce subjectivity and improve reproducibility.

Reproducibility gaps

Reproducibility in CSCR deep learning studies is limited: only 18% shared code or Model weights, and a Mere 6% made any data publicly available. This lack of transparency hinders independent verification and clinical benchmarking. Future studies should embrace open science practices, including sharing de-identified datasets, trained models, and implementation code under proper governance, to facilitate reproducibility and accelerate real-world translation.

Clinical and technical implications

Performance and Practical Limitations: A substantial proportion of studies (34%) exhibit high-risk biases, suggesting that reported metrics, such as ResNet-50 achieving 94.2% multiclass accuracy (Table 3), may overstate real-world performance. Models trained on imbalanced datasets are particularly vulnerable, often underperforming on rare subtypes. OCT excels in binary classification (Table 2) but struggles in dense cataract or complex cases, highlighting the need for multimodal integration. Advanced architectures, including Vision Transformers and multimodal fusion models, show promise but demand substantial computational resources and large annotated datasets. Lightweight models, potentially enhanced by self-supervised or transfer learning, are needed to translate laboratory success into broadly deployable clinical tools.

Conclusion

This review underscores the substantial potential of deep learning to enhance CSCR diagnosis, prognostication, and differential discrimination. Key insights include the superiority of OCT-based models, which achieve near-perfect binary classification (e.g., DenseNet: 99.78%) [96] and segmentation (Dice: 0.965), outperforming CFP-based approaches. Fusion models that combine CNNs with statistical classifiers or transformer architectures improve multiclass classification and prognostic accuracy. Clinically, segmentation of SRF/PED, differential diagnosis tools (e.g., Swin-Poly Transformer), and prognostic models (e.g., DeepPDT-Net) provide actionable information for personalized treatment planning. For the future research and clinical translation, priorities include:

- Large, diverse, multicenter datasets: Collaborate across institutions to capture acute, chronic, and atypical CSCR subtypes with multimodal imaging (OCT, FFA, ICGA, OCTA).
- Robust external validation: Test models on independent, stratified cohorts; report confidence intervals and performance on held-out centers.
- Multimodal fusion and personalized care: Combine imaging features with patient-level data (age, sex, corticosteroid exposure, symptom duration, comorbidities, smoking status, family history, metabolic markers) to support individualized prognostication.
- Interpretability and ethics: Integrate tools such as Grad-CAM, SHAP, attention maps, or VQA to clarify decision logic, detect biases, and build clinician trust.
- Harmonized data capture and missing-data handling: Adopt standardized acquisition protocols and common data models (OMOP, ICD codes); address incomplete records with model-aware imputation or mask-aware layers.
- Temporal alignment and ablation studies: Synchronize longitudinal clinical data with imaging and systematically assess the contribution of each modality or variable.
- Open science: Promote public release of code, trained models, and de-identified datasets.
- Integration and clinical workflow: Ensure seamless connectivity with PACS/EHR systems and prioritize user-friendly interfaces.
- Ethical and regulatory compliance: Address patient privacy, data security, and algorithmic bias, leveraging approaches such as federated learning to enable multi-center, privacy-preserving training.

By emphasizing data diversity, rigorous validation, interpretability, multimodal integration, and collaborative frameworks, these strategies can bridge the gap between algorithmic innovation and safe, effective, real-world deployment of AI-driven CSCR tools.

Abbreviations

CSCR	Central serous chorioretinopathy
AMD	Age-related Macular Degeneration
DR	Diabetic Retinopathy
RVO	Retina Vein Occlusion
PNV	Pachychoroid Neovasculopathy
PCV	Polypoidal Choroidal Vasculopathy
DME	Diabetic Macular Edema
CNV	Choroidal Neovascularization
VKH	Vogt-Koyanagi-Harada disease
ON	Optic Neuritis
ION	Ischemic Optic Neuropathy
RPE	Retinal Pigment Epithelium
BRB	Blood-Retina Barrier
SRF	Subretinal Fluid
SRD	Serous retinal detachment

PED	Pigment Epithelial Detachment
OCT	Optical coherence tomography
OCTA	Optical coherence tomography angiography
SS-OCT	Swept-source OCT
CFP	Color fundus photography
FFA	Fundus Fluorescein angiography
FAF	Fundus autofluorescence
ICGA	Indocyanine green angiography
BWFA	Blue-Wavelength Fundus Autofluorescence
AI	Artificial Intelligence
DL	Deep Learning
XAI	Explainable AI
CNN	Convolutional neural network
ViT	Vision Transformer
GAN	Generative adversarial networks
FSL	Few-Shot Learning
ACO	Ant colony optimization
MLT	Multi label training
FCN	Fully connected Network
FPN	Feature Pyramid Network
DWT	Discrete wavelet transform
LBP	Local binary patterns
RF	Random forests
SVM	Support vector machines
LR	Logistic regression
RoB	Risk-of-bias
QUADAS	Quality Assessment of Diagnostic Accuracy Studies
AUC-ROC	Area under the Receiver Operating Characteristic Curve
TP	True positive
TN	True Negative
FP	False positive
FN	False Negative
IEEE	Institute of Electrical and Electronics Engineers

Supplementary Information

The online version contains supplementary material available at https://doi.org/10.1186/s12886-025-04372-6.

Supplementary Material 1.

Supplementary Material 2.

Acknowledgements

Request for Waiver of Article Processing Charge (APC) for Submitted ManuscriptI hope this message finds you well. I am writing to kindly request a waiver of the Article Processing Charge (APC) for my submitted manuscript, titled "A Comprehensive Overview: Deep Learning Approaches to Central Serous Chorioretinopathy Diagnosis ", to the International Journal of BMC Ophthalmology.As a researcher deeply committed to advancing knowledge in the field of ophthalmology, my work aligns closely with the journal's mission of disseminating impactful and accessible scientific research. However, due to financial constraints compounded by international sanctions, I am currently unable to process payments, including the APC. This situation renders it impossible for me to fulfill the payment requirement, despite my earnest intent to contribute to the journal.My research investigates "innovative deep learning approaches for detection of retinal diseases", which I believe will make a valuable contribution to the field. By waiving the APC, the journal would enable the dissemination of this work to the broader scientific community, fostering innovation and collaboration in line with its commitment to accessibility and excellence.I assure you of my willingness to comply with all editorial and publication processes and my gratitude for any assistance you can provide in this matter. Your understanding and support will not only facilitate the publication of this manuscript but also affirm the journal's dedication to supporting researchers facing financial and geopolitical challenges.Thank you for considering my request. I appreciate your time and effort in reviewing this matter.Warm regards, Hamid Moghaddasi Professor in Health Information Management and Medical InformaticsDepartment of Health Information Technology and Management, School of Allied Medical SciencesShahid Beheshti University of Medical Sciences (SBMU)Darband Steet Tehran, Tehran, 1971653313, IranEmail: moghaddasi@sbmu.ac.irMobile Phone: +989123843990.

Authors' contributions

Conceptualization, Hamid moghaddasi, Mostafa Naderi, Bardia Baloutch and Mohammad Sho-jaeinia; methodology, Hamid moghaddasi, Mohammad Shokoohi yekta, and Mohammad Sho-jaeinia.; validation, Hamid Moghaddasi., Mohammad Shokoohi yekta and Mostafa Naderi.; data curation, Bardia Baloutch., Mohammad Shojaeinia; writing—original draft preparation, Mohammad Shojaeinia, and Bardia Baloutch.; writing—review and editing, Leila Akbarpour, Hamid Moghaddasi, Azam Sadat Hoseini.; visualization, Mohammad Shojaeinia.; supervision, Mostafa naderi, Hamid Moghaddasi, Azam Sadat Hoseini.; All authors have read and agreed to the published version of the manuscript.

Funding

This research received no external funding.

Data availability

No datasets were generated or analysed during the current study.

Declarations

Ethics and consent to participate

Not applicable.

Competing interests

We confirm that this manuscript has not been published elsewhere and is not under consideration by another journal. All authors have approved the manuscript and agreed to its submission. No conflicts of interest are present concerning this manuscript.

Author details

[1]Department of Health Information Technology and Management, School of Allied Medical Sciences, Shahid Beheshti University of Medical Sciences, Darband Street, Tehran 1971653313, Iran
[2]Department of Ophthalmology, Bina Eye Hospital, Tehran, Iran
[3]TRUST/FALCON RAY Imaging (X-Ray and Visible Spectrum), Tehran, Iran
[4]Head of AI, Bioxytech Retina Inc, Richmond, CA, USA
[5]Department of Foreign Languages, Shiraz Branch, Islamic Azad University, Shiraz, Fars, Iran

Received: 4 June 2025 / Accepted: 1 September 2025
Published online: 06 October 2025

References

1. Spaide RF, Campeas L, Haas A, Yannuzzi LA, Fisher YL, Guyer DR, et al. Central serous chorioretinopathy in younger and older adults. Ophthalmology. 1996;103(12):2070–80. https://doi.org/10.1016/s0161-6420(96)30386-2.
2. Song IS, Shin YU, Lee BR. Time-Periodic characteristics in the morphology of idiopathic central serous chorioretinopathy evaluated by volume scan using Spectral-Domain optical coherence tomography. Am J Ophthalmol. 2012;154(2):366–e3754.
3. van Rijssen TJ, van Dijk EHC, Yzer S, Ohno-Matsui K, Keunen JEE, Schlingemann RO, et al. Central serous chorioretinopathy: towards an evidence-based treatment guideline. Prog Retin Eye Res. 2019;73:100770.
4. Hassan SA, Akbar S, Rehman A, Saba T, Kolivand H, Bahaj SA. Recent developments in detection of central serous retinopathy through imaging and artificial intelligence techniques–a review. IEEE Access. 2021;9(3108395):168731–48.
5. Berger L, Bühler V, Yzer S. Central serous chorioretinopathy - an overview. Klin Monbl Augenheilkd. 2021;238(9):971–9. https://doi.org/10.1055/a-1531-5605.
6. Kitzmann AS, Pulido JS, Diehl NN, Hodge DO, Burke JP. The incidence of central serous chorioretinopathy in Olmsted County, Minnesota, 1980–2002. Ophthalmology. 2008;115(1):169–73.
7. Savastano MC, Dansingani KK, Rispoli M, Virgili G, Savastano A, Freund KB, et al. Classification of Haller vessel arrangements in acute and chronic central serous chorioretinopathy imaged with en face optical coherence

tomography. Retina. 2018;38(6):1211–5. https://doi.org/10.1097/iae.0000000000001678.
8. Varghese J, Kesharwani D, Parashar S, Agrawal P. A review of central serous chorioretinopathy: clinical presentation and management. Cureus. 2022;14(8):e27965.
9. Daruich A, Matet A, Dirani A, Bousquet E, Zhao M, Farman N, et al. Central serous chorioretinopathy: recent findings and new physiopathology hypothesis. Prog Retin Eye Res. 2015;48:82–118.
10. Ranjan R, Manayath G, Karandikar S, Shah V, Saravanan V, Narendran V. Central serous chorioretinopathy: current update on management. Oman J Ophthalmol. 2018;11(3):200.
11. Liew G, Quin G, Gillies M, Fraser-Bell S. Central serous chorioretinopathy: a review of epidemiology and pathophysiology. Clin Exp Ophthalmol. 2012;41(2):201–14.
12. Mohabati D, van Rijssen TJ, van Dijk E, Luyten G, Missotten TO, Hoyng C, et al. Clinical characteristics and long-term visual outcome of severe phenotypes of chronic central serous chorioretinopathy. Clin Ophthalmol. 2018;12(160956):1061–70.
13. Chronopoulos A, Kakkassery V, Strobel MA, Fornoff L, Hattenbach LO. The significance of pigment epithelial detachment in central serous chorioretinopathy. Eur J Ophthalmol. 2020;31(2):556–65.
14. Singh SR, Vaidya H, Borrelli E, Chhablani J. Foveal photoreceptor disruption in ocular diseases: an optical coherence tomography-based differential diagnosis. Surv Ophthalmol. 2023;68(4):655–68.
15. Cunha-Vaz J, Coscas G. Diagnosis of macular edema. Ophthalmologica. 2010;224(Suppl 1):2–7.
16. Cardillo Piccolino F, Lupidi M, Cagini C, Fruttini D, Nicolò M, Eandi CM, et al. Choroidal vascular reactivity in central serous chorioretinopathy. Invest Ophthalmol Vis Sci. 2018;59(10):3897.
17. Althnian A, AlSaeed D, Al-Baity H, Samha A, Dris AB, Alzakari N, et al. Impact of dataset size on classification performance: an empirical evaluation in the medical domain. Appl Sci. 2021;11(2):796.
18. Cho SC, Ryoo NK, Ahn J, Woo SJ, Park KH. Association of irregular pigment epithelial detachment in central serous chorioretinopathy with genetic variants implicated in age-related macular degeneration. Sci Rep. 2020. https://doi.org/10.1038/s41598-020-57747-8.
19. Chen M, Jin K, You K, Xu Y, Wang Y, Yip CC, et al. Automatic detection of leakage point in central serous chorioretinopathy of fundus fluorescein angiography based on time sequence deep learning. Graefes Arch Clin Exp Ophthalmol. 2021;259(8):2401–11.
20. Yoon J, Han J, Ko J, Choi S, Park JI, Hwang JS, et al. Developing and evaluating an AI-based computer-aided diagnosis system for retinal disease: diagnostic study for central serous chorioretinopathy. J Med Internet Res. 2023;25(e48142):e48142.
21. Mrejen S, Balaratnasingam C, Kaden TR, Bottini A, Dansingani K, Bhavsar KV, et al. Long-term visual outcomes and causes of vision loss in chronic central serous chorioretinopathy. Ophthalmology. 2019;126(4):576–88.
22. James AP, Dasarathy BV. Medical image fusion: A survey of the state of the Art. Inform Fusion. 2014;19(S1566253513001450):4–19.
23. Fujimoto J, Huang D. Foreword: 25 years of optical coherence tomography. Invest Ophthalmol Vis Sci. 2016;57(9):OCTi. https://doi.org/10.1167/iovs.16-20269.
24. Zheng F, Deng X, Zhang Q, He J, Ye P, Liu S, et al. Advances in swept-source optical coherence tomography and optical coherence tomography angiography. Advances in Ophthalmology Practice and Research. 2023;3(2):67–79.
25. Vira J, Marchese A, Singh RB, Agarwal A. Swept-source optical coherence tomography imaging of the retinochoroid and beyond. Expert Rev Med Devices. 2020;17(5):413–26.
26. Panwar N, Huang P, Lee J, Keane PA, Chuan TS, Richhariya A, et al. Fundus photography in the 21st century, a review of recent technological advances and their implications for worldwide healthcare. Telemedicine and e-Health. 2016;22(3):198–208.
27. Lee WJ, Lee JH, Lee BR. Fundus autofluorescence imaging patterns in central serous chorioretinopathy according to chronicity. Eye. 2016;30(10):1336–42.
28. Spaide R, Klancnikjr J. Fundus autofluorescence and central serous chorioretinopathy. Ophthalmology. 2005;112(5):825–33.
29. Eandi CM, Ober M, Iranmanesh R, Peiretti E, Yannuzzi LA. Acute central serous chorioretinopathy and fundus autofluorescence. Retina. 2005;25(8):989–93.
30. Dinc UA, Tatlipinar S, Yenerel M, Görgün E, Ciftci F. Fundus autofluorescence in acute and chronic central serous chorioretinopathy. Clin Exp Optom. 2011;94(5):452–7.
31. Zola M, Chatziralli I, Menon D, Schwartz R, Hykin P, Sivaprasad S. Evolution of fundus autofluorescence patterns over time in patients with chronic central serous chorioretinopathy. Acta Ophthalmol. 2018;96(7):e835–e839.
32. Gajdzik-Gajdecka U, Dorecka M, Nita E, Michalska A, Miniewicz-Kurowska J, Romaniuk W. Indocyanine green angiography in chronic central serous chorioretinopathy. Med Sci Monit. 2012;18(2):CR51–7.
33. Pauleikhoff LJB, Diederen RMH, Chang-Wolf JM, Moll AC, Schlingemann RO, van Dijk EHC, et al. Choroidal vascular changes on ultrawidefield indocyanine green angiography in central serous chorioretinopathy. Ophthalmol Retina. 2024;8(3):254–63.
34. Hussain N, Baskar A, Ram LM, Das T. Optical coherence tomographic pattern of fluorescein angiographic leakage site in acute central serous chorioretinopathy. Clin Exp Ophthalmol. 2006;34(2):137–40.
35. Erikitola OC, Crosby-Nwaobi R, Lotery AJ, Sivaprasad S. Photodynamic therapy for central serous chorioretinopathy. Eye. 2014;28(8):944–57.
36. Costanzo E, Cohen SY, Miere A, Querques G, Capuano V, Semoun O, et al. Optical coherence tomography angiography in central serous chorioretinopathy. J Ophthalmol. 2015;2015(134783):1–10.
37. Hu J, Qu J, Piao Z, Yao Y, Sun G, Li M, et al. Optical coherence tomography angiography compared with indocyanine green angiography in central serous chorioretinopathy. Sci Rep. 2019. https://doi.org/10.1038/s41598-019-42623-x.
38. M DS, K AN, B MA. En face optical coherence tomography transillumination for evaluation of retinal pigment epithelium alteration in central serous chorioretinopathy: correlation with multimodal imaging. Graefe's Archive Clin Experimental Ophthalmol. 2022;260(7):2231–7.
39. Yoon J, Han J, Park JI, Hwang JS, Han JM, Sohn J, et al. Optical coherence tomography-based deep-learning model for detecting central serous chorioretinopathy. Sci Rep. 2020. https://doi.org/10.1038/s41598-020-75816-w.
40. Hagag AM, Chandra S, Khalid H, Lamin A, Keane PA, Lotery AJ, et al. Multimodal imaging in the management of choroidal neovascularization secondary to central serous chorioretinopathy. J Clin Med. 2020;9(6):1934.
41. Yeo JH, Oh R, Kim YJ, Kim JG, Yoon YH, Lee JY. Choroidal neovascularization secondary to central serous chorioretinopathy: OCT angiography findings and risk factors. J Ophthalmol. 2020;2020(7217906):1–9.
42. Khan A, Pin K, Aziz A, Han JW, Nam Y. Optical coherence tomography image classification using hybrid deep learning and ant colony optimization. Sensors. 2023;23(15):6706.
43. Gende M, Castelo L, de Moura J, Novo J, Ortega M. Intra- and inter-expert validation of an automatic segmentation method for fluid regions associated with central serous chorioretinopathy in OCT images. Journal of Imaging Informatics in Medicine. 2024;37(1):107–22.
44. Jee D, Yoon JH, Ra H, Kwon Jwoo, Baek J. Predicting persistent central serous chorioretinopathy using multiple optical coherence tomographic images by deep learning. Sci Rep. 2022. https://doi.org/10.1038/s41598-022-13473-x.
45. Hassan SAE, Akbar S, Gull S, Rehman A, Alaska H. Deep Learning-Based Automatic Detection of Central Serous Retinopathy using Optical Coherence Tomographic Images. In: 2021 1st International Conference on Artificial Intelligence and Data Analytics (CAIDA) [Internet]. IEEE; 2021 [cited 2025 Jun 12]. pp. 206–11. Available from: https://doi.org/10.1109/caida51941.2021.9425161
46. Xu J, Shen J, Wan C, Yan Z, Zhou F, Zhang S, et al. An automatic image processing method based on artificial intelligence for locating the key boundary points in the central serous chorioretinopathy lesion area. Comput Intell Neurosci. 2023;2023:1839387.
47. Gawęcki M, Grzybowski A. Ganglion cell loss in the course of central serous chorioretinopathy. Ophthalmol Ther. 2022;12(1):517–33.
48. He J, Wang J, Han Z, Ma J, Wang C, Qi M. An interpretable transformer network for the retinal disease classification using optical coherence tomography. Sci Rep. 2023. https://doi.org/10.1038/s41598-023-30853-z.
49. Liu W, Zhang J, Zhao Y. A Comparison of Deep Learning and Traditional Machine Learning Approaches in Detecting Cognitive Impairment Using MRI Scans. In: 2022 IEEE 46th Annual Computers, Software, and Applications Conference (COMPSAC). IEEE; 2022 Cited 12 Jun 2025. pp. 998–1001. Available from: https://doi.org/10.1109/compsac54236.2022.00154.
50. Opoku M, Weyori BA, Adekoya AF, Adu K. Clahe-CapsNet: efficient retina optical coherence tomography classification using capsule networks with contrast-limited adaptive histogram equalization. PLoS ONE. 2023;18(11):e0288663.
51. Goodfellow I, Bengio Y, Courville A. Deep learning. Cambridge: MIT Press; 2016.

52. Ting DSW, Pasquale LR, Peng L, Campbell JP, Lee AY, Raman R, et al. Artificial intelligence and deep learning in ophthalmology. Br J Ophthalmol. 2018;103(2):167–75.
53. Yamashita R, Nishio M, Do RKG, Togashi K. Convolutional neural networks: an overview and application in radiology. Insights into Imaging. 2018;9(4):611–29.
54. Litjens G, Kooi T, Bejnordi BE, Setio AAA, Ciompi F, Ghafoorian M, et al. A survey on deep learning in medical image analysis. Med Image Anal. 2017;42(S1361841517301135):60–88.
55. Liu X, Faes L, Kale AU, Wagner SK, Fu DJ, Bruynseels A, et al. A comparison of deep learning performance against health-care professionals in detecting diseases from medical imaging: a systematic review and meta-analysis. Lancet Digit Health. 2019;1(6):e271–97.
56. Shen D, Wu G, Suk HI. Deep learning in medical image analysis. Annu Rev Biomed Eng. 2017;19(1):221–48.
57. Moher D, Liberati A, Tetzlaff J, Altman DG. Preferred reporting items for systematic reviews and meta-analyses: the PRISMA statement. PLoS Med. 2009;6(7):e1000097.
58. Esteva A, Robicquet A, Ramsundar B, Kuleshov V, DePristo M, Chou K, et al. A guide to deep learning in healthcare. Nat Med. 2019;25(1):24–9.
59. Pawan SJ, Sankar R, Jain A, Jain M, Darshan DV, Anoop BN, et al. Capsule network–based architectures for the segmentation of sub-retinal serous fluid in optical coherence tomography images of central serous chorioretinopathy. Med Biol Eng Comput. 2021;59(6):1245–59.
60. Xu J, Yang W, Wan C, Shen J. Weakly supervised detection of central serous chorioretinopathy based on local binary patterns and discrete wavelet transform. Comput Biol Med. 2020;127:104056.
61. Xu F, Wan C, Zhao L, You Q, Xiang Y, Zhou L, et al. Predicting central serous chorioretinopathy recurrence using machine learning. Front Physiol. 2021;12:649316.
62. Yoo TK, Kim BY, Jeong HK, Kim HK, Yang D, Ryu IH. Simple code implementation for deep learning–based segmentation to evaluate central serous chorioretinopathy in fundus photography. Transl Vis Sci Technol. 2022;11(2):22.
63. Aoyama Y, Maruko I, Kawano T, Yokoyama T, Ogawa Y, Maruko R, et al. Diagnosis of central serous chorioretinopathy by deep learning analysis of en face images of choroidal vasculature: a pilot study. PLoS ONE. 2021;16(6):e0244469.
64. Xu F, Liu S, Xiang Y, Lin Z, Li C, Zhou L, et al. Deep learning for detecting subretinal fluid and discerning macular status by fundus images in central serous chorioretinopathy. Front Bioeng Biotechnol. 2021;9:651340.
65. Nelson B, Pandiyapallil Abdul Khadir H, Odattil S. Detection of CSR from blue wave fundus autofluorescence images using deep neural network based on transfer learning. International journal of electrical and computer engineering systems. 2023;14(3):277–84.
66. Zhou C, Zhang T, Chen L, Wen Y, Lei T, Chen J. Attention-Based Detection for Central Serious Chorioretinopathy in Fundus Image. In: 2020 IEEE International Conference on Bioinformatics and Biomedicine (BIBM). IEEE; 2020 Cited 12 Jun 2025. pp. 1221–5. Available from: https://doi.org/10.1109/bibm49941.2020.9313400.
67. Zhen Y, Chen H, Zhang X, Meng X, Zhang J, Pu J, ASSESSMENT OF CENTRAL SEROUS CHORIORETINOPATHY DEPICTED ON COLOR FUNDUS PHOTOGRAPHS USING DEEP LEARNING. Retina. 2020;40(8):1558–64.
68. Üzen H, Fırat H, Alperen Özçelik ST, Yusufoğlu E, Çiçek İB, Şengür A. Central serous retinopathy classification with deep learning-based multilevel feature extraction from optical coherence tomography images. Opt Laser Technol. 2025;184:112519.
69. Ko J, Han J, Yoon J, Park JI, Hwang JS, Han JM, et al. Assessing central serous chorioretinopathy with deep learning and multiple optical coherence tomography images. Sci Rep. 2022. https://doi.org/10.1038/s41598-022-05051-y.
70. de Moura J, Novo J, Ortega M, Barreira N, Penedo MG. Automated Segmentation of the Central Serous Chorioretinopathy fluid regions using Optical Coherence Tomography Scans. In: 2021 IEEE 34th International Symposium on Computer-Based Medical Systems (CBMS). IEEE; 2021 Cited 12 Jun 2025. pp. 1–6. Available from: https://doi.org/10.1109/cbms52027.2021.00008.
71. Narendra Rao TJ, Girish GN, Kothari AR, Rajan J. Deep Learning Based Sub-Retinal Fluid Segmentation in Central Serous Chorioretinopathy Optical Coherence Tomography Scans. Annu Int Conf IEEE Eng Med Biol Soc. 2019;2019:978–981. https://doi.org/10.1109/EMBC.2019.8857105. PMID: 31946057.
72. Xu J, Shen J, Wan C, Jiang Q, Yan Z, Yang W. A few-shot learning-based retinal vessel segmentation method for assisting in the central serous chorioretinopathy laser surgery. Front Med. 2022;9:821565.
73. Burlina PM, Joshi N, Pekala M, Pacheco KD, Freund DE, Bressler NM. Automated grading of age-related macular degeneration from color fundus images using deep convolutional neural networks. JAMA Ophthalmol. 2017;135(11):1170.
74. Ting DSW, Cheung CYL, Lim G, Tan GSW, Quang ND, Gan A, et al. Development and validation of a deep learning system for diabetic retinopathy and related eye diseases using retinal images from multiethnic populations with diabetes. JAMA. 2017;318(22):2211.
75. Gulshan V, Peng L, Coram M, Stumpe MC, Wu D, Narayanaswamy A, et al. Development and validation of a deep learning algorithm for detection of diabetic retinopathy in retinal fundus photographs. JAMA. 2016;316(22):2402.
76. Bonini Filho MA, de Carlo TE, Ferrara D, Adhi M, Baumal CR, Witkin AJ, et al. Association of choroidal neovascularization and central serous chorioretinopathy with optical coherence tomography angiography. JAMA Ophthalmol. 2015;133(8):899.
77. Hayreh SS. Ischemic optic neuropathy. Prog Retin Eye Res. 2009;28(1):34–62.
78. Bennett JL. Optic neuritis. CONTINUUM: Lifelong Learn Neurol. 2019;25(5):1236–64.
79. Shields JA, Shields CL. Intraocular tumors: an atlas and textbook. Lippincott Williams & Wilkins; 2008.
80. Wen Y, Chen L, Qiao L, Deng Y, Dai S, Chen J, On Automatic Detection of Central Serous Chorioretinopathy and Central Exudative Chorioretinopathy in Fundus Images. In:, Bioinformatics et al. and Biomedicine (BIBM). IEEE; 2020 Cited 12 Jun 2025. pp. 1161–5. Available from: https://doi.org/10.1109/bibm49941.2020.9313274.
81. Rodríguez MA, AlMarzouqi H, Liatsis P. Multi-label retinal disease classification using transformers. IEEE J Biomed Health Inform. 2023;27(6):2739–50.
82. Yoo TK, Kim SH, Kim M, Lee CS, Byeon SH, Kim SS, et al. Deeppdt-net: predicting the outcome of photodynamic therapy for chronic central serous chorioretinopathy using two-stage multimodal transfer learning. Sci Rep. 2022. https://doi.org/10.1038/s41598-022-22984-6.
83. Fernández-Vigo JI, Gómez Calleja V, de Moura Ramos JJ, Novo-Bujan J, Burgos-Blasco B, López-Guajardo L, et al. Prediction of the response to photodynamic therapy in patients with chronic central serous chorioretinopathy based on optical coherence tomography using deep learning. Photodiagnosis Photodyn Ther. 2022. https://doi.org/10.1016/j.pdpdt.2022.103107.
84. Abouammoh MA. Advances in the treatment of central serous chorioretinopathy. Saudi J Ophthalmol. 2015;29(4):278–86.
85. Xu F, Wan C, Zhao L, Liu S, Hong J, Xiang Y, et al. Predicting post-therapeutic visual acuity and OCT images in patients with central serous chorioretinopathy by artificial intelligence. Front Bioeng Biotechnol. 2021;9:649221.
86. Yoon J, Han J, Ko J, Choi S, Park JI, Hwang JS, et al. Classifying central serous chorioretinopathy subtypes with a deep neural network using optical coherence tomography images: a cross-sectional study. Sci Rep. 2022. https://doi.org/10.1038/s41598-021-04424-z.
87. Al-hammuri K, Gebali F, Kanan A, Chelvan IT. Vision transformer architecture and applications in digital health: a tutorial and survey. Vis Comput Ind Biomed Art. 2023;6(1):14.
88. Jiang Z, Wang L, Wu Q, Shao Y, Shen M, Jiang W, et al. Computer-aided diagnosis of retinopathy based on vision transformer. J Innov Opt Health Sci. 2022. https://doi.org/10.1142/S1793545822500092.
89. Lange CA, Qureshi R, Pauleikhoff L. Interventions for central serous chorioretinopathy: a network meta- analysis. Cochrane Database Syst Reviews. 2025;2025(6). https://doi.org/10.1002/14651858.cd011841.pub3.
90. Santarossa M, Tatli A, von der Burchard C, Andresen J, Roider J, Handels H, et al. Chronological registration of OCT and autofluorescence findings in CSCR: two distinct patterns in disease course. Diagnostics. 2022;12(8):1780.
91. Zhang X, Lim CZF, Chhablani J, Wong YM. Central serous chorioretinopathy: updates in the pathogenesis, diagnosis, and therapeutic strategies. Eye Vis. 2023. https://doi.org/10.1186/s40662-023-00349-y.
92. Shorten C, Khoshgoftaar TM. A survey on image data augmentation for deep learning. J Big Data. 2019;6(1):60.
93. Seiler E, Delachaux L, Cattaneo J, Garjani A, Duriez A, Martin T et al. Importance of OCT-derived Biomarkers for the Recurrence of Central Serous Chorioretinopathy using Statistics and Predictive Modelling. Springer Science and Business Media LLC; 2024 Mar Cited 17 Aug 2025. Available from: https://doi.org/10.21203/rs.3.rs-4170618/v1.
94. Caplash S, Surakiatchanukul T, Arora S, Maltsev DS, Singh SR, Sahoo NK, et al. Multimodal imaging-based predictors for the development of choroidal

neovascularization in patients with central serous chorioretinopathy. J Clin Med. 2023;12(5):2069.
95. Bousquet E, Torres-Villaros H, Provost J, Elalouf M, Gigon A, Mantel I, et al. Clinical characteristics and multimodal imaging findings of central serous chorioretinopathy in women versus men. J Clin Med. 2022. https://doi.org/10.3390/jcm11061706.
96. Hassan SA, Akbar S, Khan HU. Detection of central serous retinopathy using deep learning through retinal images. Multimedia Tools Appl. 2023;83(7):21369–96.

Publisher's Note